Applied Energy 347 (2023) 121440

Contents lists available at ScienceDirect

Applied Energy

journal homepage: www.elsevier.com/locate/apenergy

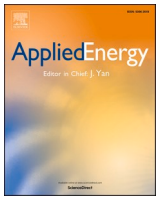

A three-layer game theoretic-based strategy for optimal scheduling of microgrids by leveraging a dynamic demand response program designer to unlock the potential of smart buildings and electric vehicle fleets

Seyed Amir Mansouri [a,*], Ángel Paredes [b], José Manuel González [b], José A. Aguado [b]

[a] Institute for Research in Technology (IIT), ICAI School of Engineering, Comillas Pontifical University, 28015 Madrid, Spain
[b] Department of Electrical Engineering, Escuela de Ingenierías Industriales, University of Málaga, 29071 Málaga, Spain

HIGHLIGHTS

- Providing a RA three-layer strategy for DA scheduling of an AND consisting of multiple MGs.
- Reducing the daily expenses of ADN through the design of a dynamic-tariff DRP.
- Improving the technical and economic metrics of the ADN by unlocking the potential of SBs and EV fleets.
- Improving the equilibrium point of the DA scheduling of MGs through the game theory and the P2P power sharing.

ARTICLE INFO

Keywords:
Microgrids
Cooperative game theory
Smart buildings
Vehicle-to-grid services
Demand response programs
Temperature Comfort

ABSTRACT

The proliferation of the number of Smart Buildings (SBs) and the fleet of Electric Vehicles (EVs) in Distribution Systems (DSs) makes the need for new strategies to coordinate them with microgrid (MG) scheduling inevitable. Therefore, this article proposes a three-layer risk-averse game theoretic-based strategy to coordinate SBs and EV fleets with MGs scheduling. In the first layer of this strategy, a Demand Response Program (DRP) is designed for SBs where dynamic incentive tariffs are calculated based on the consumption pattern of subscribers. Then, in the second layer, the scheduling of SBs and EV fleets is done in a decentralized space and considering their participation in the designed DRP. Eventually, in the third layer, the operators of MGs have received the power exchange information of SBs in order to carry out their scheduling in accordance with it. In this layer, the Day-Ahead (DA) scheduling of MGs and DS is done through the implementation of a cooperative game theory. Fluctuations of uncertain operational parameters such as load demand, radiation and wind are embedded in the model by scenario-based technique where a Risk-Averse (RA) strategy is adopted to manage them. Running the proposed three-layer strategy on a 69-node DS containing four MGs showed that this strategy can use the potential of SBs and EV fleets to improve the voltage characteristics in the high-demand period and reduce total daily costs by 13.66% with designing a dynamic-tariff DRP. Moreover, the results reveal that MGs using the Peer-to-Peer (P2P) power exchange option have not only reduced the power losses in the system but also reduced the total daily costs by about 8%.

1. Introduction

1.1. Background and motivation

The ever-increasing demand of electrical energy systems alongside with the net zero emissions objectives is given rise to a profound change in the paradigm of the electricity generation and mobility [1]. Sustainable objectives can no longer be deferred, forming a vertical part of the objectives, the planning, and the operation of the electrical energy systems. In this sense, MGs are well suited for the management of this growing demand. Distributed generation can be easily accommodated near the location of the demand using multiple renewable generation technologies, i.e., PV panels and Wind Turbines (WT). Besides, small to medium scale distributed Battery Energy Storages (BESs) can be integrated in those systems, which increases the flexibility of the MGs. On

* Corresponding author.
E-mail addresses: smansouri@comillas.edu, amir.mansouri24@gmail.com (S.A. Mansouri).

https://doi.org/10.1016/j.apenergy.2023.121440
Received 10 March 2023; Received in revised form 26 April 2023; Accepted 10 June 2023

Nomenclature

Abbreviations

AC	Air Conditioning
ADN	Active Distribution Network
BES	Battery Energy Storage
DA	Day-Ahead
DRP	Demand Response Program
EV	Electric Vehicle
EWH	Electric Water Heater
MG	Microgrid
RA	Risk-Averse
SB	Smart Building
TC	Temperature Comfort
V2G	Vehicle to Grid
WT	Wind Turbine

Sets

b	SB index
e	BES index
ev	EV index
g	GT index
i,j	Node index
l	Branch index
m,n	MG index
pv	PV system index
sc	Scenario index
t	Time index
w	WT index

Scalars

α^{AC}	AC thermal performance factor (°C/kWh)
α^{B}	Thermal constant of building
α^{R}	Weight of variable reward
β	Confidence Level (%)
δ	Cost deviation factor
Δt	Time step (h)
Δx	Insulation thickness (m)
ε	Reward damping factor
η^{Ch}/η^{Dis}	Charge/Discharge efficiency of BES/EV (%)
η^{PV}	Efficiency of photovoltaic system (%)
G^{STC}	Standard sun irradiance (W/m^2)
γ^{R}	DRP base reward factor ($/kWh)
h	Surface heat transfer coefficient (W/m^{2}K)
k	Energy conversion constant (kWh/J)
κ	Thermal conductivity (W/mK)
ω	Risk averse factor (%)
p	Specific heat of water (J/kgC^o)
$S_{surface}$	Tank surface area (m^2)
$TC^{\min}$	Min temperature Comfort level (%)
τ	Temperature Comfort damping factor
T^a/T^d	Arrival/Departure Time (h)
$\theta^{W,Initial}/\theta^{B,Initial}$	Initial water/indoor temperature (C^o)
θ^{Cold}	Cold water temperature (C^o)
$\theta^{\min}/\theta^{\max}$	Min/Max voltage angle (rad)
$v_{ci}/v_r/v_{co}$	Cut-in/Rated/Cut-out wind speed (m/s)
$V^{\min}/V^{\max}$	Min/Max voltage magnitude (p.u)

Parameters

$\alpha_g^{\max}$	Max reactive power range of gas turbine (%)
Cap_e^B	Storage capacity of BES (kWh)
Cap_{ev}^{EV}	Storage capacity of EV (kWh)
$G_{t,sc}$	Sun irradiance (W/m^2)
$\gamma^{Ch,\max}/\gamma^{Dis,\max}$	Max charge/discharge level (%)
ρ_{sc}	Scenario probability (%)
$P_g^{G,\min}/P_g^{G,\max}$	Min/Max active power generation of gas turbine (kW)
$P_{b,sc}^{Avg,Load}$	Average load of building (kW)
$\overline{P}_{b,t,sc}^{Load}$	Load scenarios of building (kW)
$\widehat{P}_{b,t,sc}^{L,DR-}$	Max downward DRP (kW)
$P_{b,t}^{L,Desire}$	Preferred load profile of AC and EWH systems (kW)
$P_{w,t,sc}^{W}$	Available wind power (kW)
$P_w^{W,\max}$	Max wind power (kW)
$P_{pv,t,sc}^{PV}$	Available PV power (kW)
$P_{pv}^{PV,\max}$	Max PV power (kW)
$P^{AC,\max}$	Max power usage of AC (kW)
$P_{i,t,sc}^{Demand}/Q_{i,t,sc}^{Demand}$	Predefines active/reactive load of nodes
$\pi_{b,t,sc}^{L,DR-}$	Downward DRP reward ($/kWh)
π_t^{E}	Energy price ($/kWh)
$\pi_t^{EV,Dch}$	V2G service reward ($/kWh)
π_g^{G}	Generation price of gas turbine ($/kW)
$P_b^{EWH,\max}$	Nominal power of water heater (kWh)
R_l	Resistance of network Branch (ohm)
$S_l^{Line,\max}$	Max appearance power of network Branch (kVA)
$SOC^{B,Initial}$	Initial SoC of BES (%)
$SOC_{ev}^{EV,Initial}/SOC_{ev}^{EV,Final}$	Initial/Final SoC of EV (%)
$SOC^{\min}/SOC^{\max}$	Min/Max SoC (%)
$\theta_{b,t,sc}^{Amb}$	Ambient temperature (C^o)
$\theta_t^{W,\min}/\theta_t^{W,\max}$	Min/Max temperature of hot water (C^o)
$\theta_t^{B,\min}/\theta_t^{B,\max}$	Min/Max temperature of building (C^o)
$v_{t,sc}$	Wind speed (m/s)
$v_{b,t,sc}^{tank}$	Volume of the stored water in tank (kg)
v_b^{EWH}	Capacity of water tank (kg)
$\xi_{l,i}/\xi_{l,m}$	Flow direction factor

Variables

$\eta_{m,sc}$	Deviation from the optimum point ($)
$C_{e,t,sc}^{B}$	BES operation cost ($)
$C_{b,sc}^{Building}$	Building energy cost ($)
$C_{m,sc}^{MG}$	Microgrid operation cost ($)
$C_{g,t,sc}^{G}$	Gas turbine operation cost ($)
$CVaR_m$	Conditional value at risk ($)
φ_x	Max deviation radius of uncertain parameter
$P_{b,t,sc}^{Building}$	Building energy consumption (kW)
$P_{g,t,sc}^{G}/Q_{g,t,sc}^{G}$	Active/Reactive power generation of gas turbine (kW/kVAR)
$P_{e,t,sc}^{B,Ch}/P_{e,t,sc}^{B,Dis}$	Charge/Discharge power of BES (kW)
$P_{ev,t,sc}^{EV,Ch}/P_{ev,t,sc}^{EV,Dis}$	Charge/Discharge power of EV (kW)
$P_{l,t,sc}^{Line}/Q_{l,t,sc}^{Line}$	Active/Reactive power flow (kW)
$P_{b,t,sc}^{Load}$	Electrical load of building (kW)
$P_{b,t,sc}^{AC}$	Electrical load of AC (kW)
$P_{b,t,sc}^{EWH}$	Electrical load of EWH (kW)
$P_{b,t,sc}^{L,DR-}$	Downward DRP participation (kW)
$P_{l,t,sc}^{Loss}$	Power loss (kW)
$Q_{b,t,sc}^{EWH}$	Energy demand of hot water (kWh)
$Q_{b,t,sc}^{Loss}$	Energy loss of hot water (kWh)
$SOC_{e,t,sc}^{B}$	Level of stored energy in ESS (%)
$SOC_{ev,t,sc}^{EV}$	Level of stored energy in EV (%)
$TC_{b,sc}$	Temperature Comfort level (%)
$\theta_{b,t,sc}^{W}$	Hot water temperature (°C)

$\theta^{B}_{b,t,sc}$	Building temperature (°C)
$\theta_{i,t,sc}$	Voltage angle (rad)
VaR_m	Value at risk ($)
$V_{i,t,sc}$	Voltage magnitude (p.u)

Binary Variables

$I^{B,Ch}_{e,t,sc}/I^{B,Dis}_{e,t,sc}$	Charge/Discharge status of BES
$I^{EV,Ch}_{ev,t,sc}/I^{EV,Dis}_{ev,t,sc}$	Charge/Discharge status of EV

top of this, the electrification of heating and mobility leads to so-called SBs which can jointly manage and control Air Conditioning (ACs) systems, fleets of EVs and DRPs [2]. These SBs can be also allocated in MGs increasing their flexibility and the services they can procure. However, these MGs are limited in size, finding it hard to procure cost-effective services if multiple MGs are not integrated [3]. In this sense, Active Distribution Networks (ADNs) provide an effective framework to support the integration of multiple MGs providing different services, e.g. Vehicle to Grid (V2G) or DRPs, to the grid while meeting the programs of the final users [4]. In this setting, the efficiency of the energy system can be enhanced if those MGs cooperate among them, which motivates the study of a game theoretic based strategy for the management of multiple MGs in the context of ADNs.

1.2. Literature review

The Energy Management (EM) problem of multi-MGs has been investigated from different perspectives because of its primal importance in achieving stable, reliable, and cost-effective solutions. EM Systems (EMSs) for multi-MGs are composed of an information module which is responsible of gathering information that allows the scheduling and control module to operate efficiently [5]. In this sense, developing attractive DRPs are of vital importance to incentive the participation of different actors, which increases the flexibility of the grid. Several DRPs has been investigated in the literature. Time-based DRPs provide a time-varying price for the energy based on the needs of the system [6]. Time of use tariffs maintain different prices depending on the moment of the day of the week [7]. Peak tariffs allow the system operator to drastically increase the price when there is an eventuality in the system [8]. Another time-based DRPs in which the price is determined depending on the location of the grid and the moment of the day on a rolling horizon basis is the real time pricing [9], this tariff offers higher flexibility to the system operator. However, end-users are not incentive to lower their demand, which hinders the efficacy of this tariff. On the other hand, incentive-based programs offer bonuses to customers for their participation in DRPs [10]. Several incentive strategies are investigated, authors in [11] proposes a direct load controlling methodology where several hierarchical incentive coefficients minimize the cost of energy for residents while flattening demand. Curtailable load programs award customers that are available to reduce or even interrupt their consumption [12]. Authors in [13] propose an emergency DRP which responds to real-time emergency events with bonuses to reduce end-user consumption.

MGs can be categorized into residential, commercial, and industrial depending on the type of their final users. Generally, they include several types of Renewable Distributed Energy Resources (RDERs), such as Wind Turbines (WT), PV solar panels and BES systems [14]. SBs recently gained attraction as the fundamental block constituting MGs [15], as they can effectively manage Electric Water Heaters (EWHs) [16], solar PV based generation [17] and even Vehicle to Building (V2B) services of fleets of EVs [18].

Several strategies are implemented in the literature regarding the final aim of the EMS of the MG. Environmental costs of the operation of the MGs are minimized regarding the carbon emissions of the DERs in [19] and regarding the penalties for emissions in [20]. Other branch of research minimizes capital and operational costs of the MGs regarding fuel needs [21], investment [22] or operational costs [23]. On top of that, due to the overly importance of the BES systems, authors in [23] minimize the costs of storage systems. End user satisfaction is also considered in [24] where a methodology for reducing the dissatisfaction of the DRPs is investigated. Due to the great variety of objectives, multi-objective approaches are common. They jointly optimize several functions using epsilon-constraint method to find the pareto-optimal fronts [25]. The management of renewable generation uncertainty in these systems has profound implications. In this sense, a risk management strategy has been addressed by [26] to protect the system against the uncertainty of the RDERs. Nevertheless, other types of objectives have not been considered. A tri-level framework has been investigated in the literature for the coordination of different stakeholders. The author in [27] proposes a tri-level framework to coordinate a smart distribution network with microgrids and customers under a DRP. Then, the tri-level optimization problem is converted into a two-level problem which is coordinated using a full cooperative an ancillary services framework.

In the context of multi-MGs, game theory is used as a tool for modeling the behavior of them when implementing a DRPs or participating in markets. Authors in [28] developed a tri-level Stackelberg game model to maximize the payoff of each MG participating in wholesale markets. DRPs are implemented along with the technical and security constraints of the MGs in [29] using a bi-level cooperative game approach, while in [30] a non-cooperative game is used to solve the EM problem of MGs clusters. Additionally, an evolutionary game-theoretic approach is investigated in [31] which its non-cooperative objective aims to solve the EM of the multi-MGs using neural networks to balance each agent. On the other hand, P2P methodologies are also used for solving the EMS of multi-MGs [32], even considering the market elasticity in a community microgrid [33].

1.3. Research gaps and contributions

To compare the features of this article with recent articles, Table 1 is presented, which detailed analysis reveals that the model proposed in this article includes more cases compared to recent researches. Overall, the analysis of research articles published in recent years reveals none of the researches have addressed the effects of the joint implementation of the P2P power transaction, dynamic-tariff DRP and V2G services on the performance of cooperative game theory technique and the equilibrium point of DA scheduling of MGs. Moreover, the literature evaluation clearly reflects that there are many gaps in the discussions related to releasing the potential of SBs and EV fleets to improve the technical, economic and security aspects of the operation of multi-MGs in ADNs that need to be bridged.

The above shortcomings have encouraged the authors of this article to propose a comprehensive three-layer strategy for coordinating SBs and EV fleets with DA scheduling of MGs, where the effects of the joint implementation of RA strategy, P2P power transaction, dynamic-tariff DRP and V2G services on cooperative game theory performance, MGs daily costs, operational security and technical metrics are analyzed in detail. The contributions of the proposed strategy fulfill the limitations identified in the literature as follows:

- Providing a RA three-layer strategy for DA scheduling of an AND consisting of multiple MGs integrated with SBs, EV fleets, RERs and BES systems
- Reducing the daily expenses of ADN through the design of a dynamic-tariff DRP fully compatible with smart-users' behaviors

Table 1
Comparing the features of this article with the literature.

Refs.	MILP Modelling	Networked MGs	DRP Tariffs		P2P Power Sharing	Game Theory	Smart Prosumers	RDERs		EV Modelling		Stochastic Programing		Power Flow Program
			Static	Dynamic				WT	PV	G2V	V2G	Uncertainty	Risk Management	
[34]	x	x	✓	x	✓	✓	✓	x	✓	x	x	✓	x	x
[35]	✓	✓	x	x	x	✓	x	✓	✓	x	x	x	x	x
[36]	x	x	x	x	x	x	x	✓	✓	x	x	x	x	x
[37]	✓	✓	✓	x	x	x	✓	✓	✓	✓	✓	✓	x	✓
[38]	✓	✓	x	x	x	x	x	✓	✓	x	x	✓	x	✓
[39]	✓	✓	x	x	x	x	x	✓	✓	x	x	✓	x	✓
[40]	✓	x	x	x	x	x	x	✓	✓	✓	✓	✓	x	x
[41]	✓	x	✓	x	x	x	x	✓	✓	x	x	✓	✓	x
[42]	x	x	x	✓	x	✓	x	x	✓	x	x	✓	x	x
[43]	✓	✓	✓	x	✓	✓	x	✓	✓	x	x	✓	x	✓
[44]	✓	x	✓	x	x	x	✓	✓	✓	x	x	x	x	x
[45]	✓	x	x	x	x	x	✓	x	✓	x	x	✓	✓	x
[46]	✓	x	✓	x	x	x	x	✓	✓	✓	✓	✓	✓	x
[47]	✓	✓	x	x	x	x	x	x	✓	✓	✓	✓	x	x
[48]	✓	x	x	x	✓	x	✓	x	✓	x	x	x	x	✓
[49]	x	x	x	✓	✓	x	✓	✓	✓	✓	✓	x	x	x
[50]	x	x	x	✓	✓	✓	✓	x	✓	x	x	x	x	x
[51]	✓	✓	x	x	x	✓	x	x	✓	x	x	✓	x	✓
[52]	x	✓	x	x	x	✓	x	✓	✓	✓	✓	✓	x	✓
[53]	✓	✓	✓	x	x	✓	✓	x	✓	x	x	✓	x	✓
[54]	✓	x	x	x	x	✓	✓	✓	✓	x	x	✓	✓	x
[55]	x	x	x	✓	✓	x	✓	x	✓	✓	✓	✓	x	✓
This Work	✓	✓	✓	✓	✓	✓	✓	✓	✓	✓	✓	✓	✓	✓

- Improving the technical and economic metrics of the ADN by unlocking the potential of SBs and EV fleets using implementing a dynamic-tariff DRP
- Improving the equilibrium point of the DA scheduling of MGs through the joint implementation of the cooperative game theory and the P2P power transaction among MGs
- Covering different operating scenarios and subsequently ensuring the sustainability of energy supply through the implementation of a RA strategy

1.4. Paper organization

The remainder of the article is organized as follows. Section 2 describes the three-layer model. Section 3 provides the mathematical description of the model. The case study and the simulation results are presented in Section 4. Lastly, Section 5 concludes the paper.

2. The proposed three-layer game theoretic EM strategy

A flowchart is presented in Fig. 1 to illustrate the implementation process of the proposed three-layer EM strategy. At first, it should be pointed out that the problem is coded in GAMS space where the CPLEX solver is applied to solve it. As per this flowchart, the design of DRPs, the DA scheduling of SBs and the DA scheduling of MGs and DS are done in the first to third layers, respectively. In the first layer, the operator of each MG designs DRPs with time-varying bonuses for SBs based on their average demand for the past thirty days. In the second layer, SBs do their scheduling according to the DRPs received from the MG operator with the aim of minimizing their daily electricity bill. The output of this layer is the hourly power purchase / sale of each building, which is sent to the corresponding MG operator. Finally, in the third layer, the daily scheduling of MGs is done through the implementation of a cooperative game, considering the requested programs of SBs. The full description and the pseudocode required to implement the proposed cooperative game theory technique are provided in subsection 3.1.

It should be pointed out the parameters of load demand, sun irradiance and wind have uncertainty. Hence, 1,000 scenarios have been generated for the above-mentioned parameters through the simulation of probability distribution functions in the GAMS environment. These functions include Normal Distribution Function (NDF) to generate load scenarios, Weibull Distribution Function (WDF) to generate wind scenarios and Beta Distribution Function (BDF) to generate solar sun irradiance scenarios. After completing the scenario generation process, the number of scenarios is reduced to 20 through the ScenRed technique to reduce the solution time. Eventually, as will be explained in Section 3.1, the RA strategy is used to create a safe region for the operation for handling different DA operational scenarios.

3. Mathematical modelling

In this section the mixed-integer linear programming (MILP) modelling of the proposed three-layer DA scheduling strategy is described.

3.1. Description of the layers of the problem

- **Layer 1**

In layer 1, the MG operator designs DRPs with dynamic (time-varying) incentive tariffs for SBs. These DRPs are designed by an exponential function and with regard to the average load demand of the last thirty days of each SB. Note that this exponential function calculates DRP rewards according to the difference between the hourly load ($P^{*Load}_{b,t,sc}$) and the average load value ($P^{Avg.Load}_{b,sc}$). Therefore, this function leads to the achievement of different rewards for each hour according to

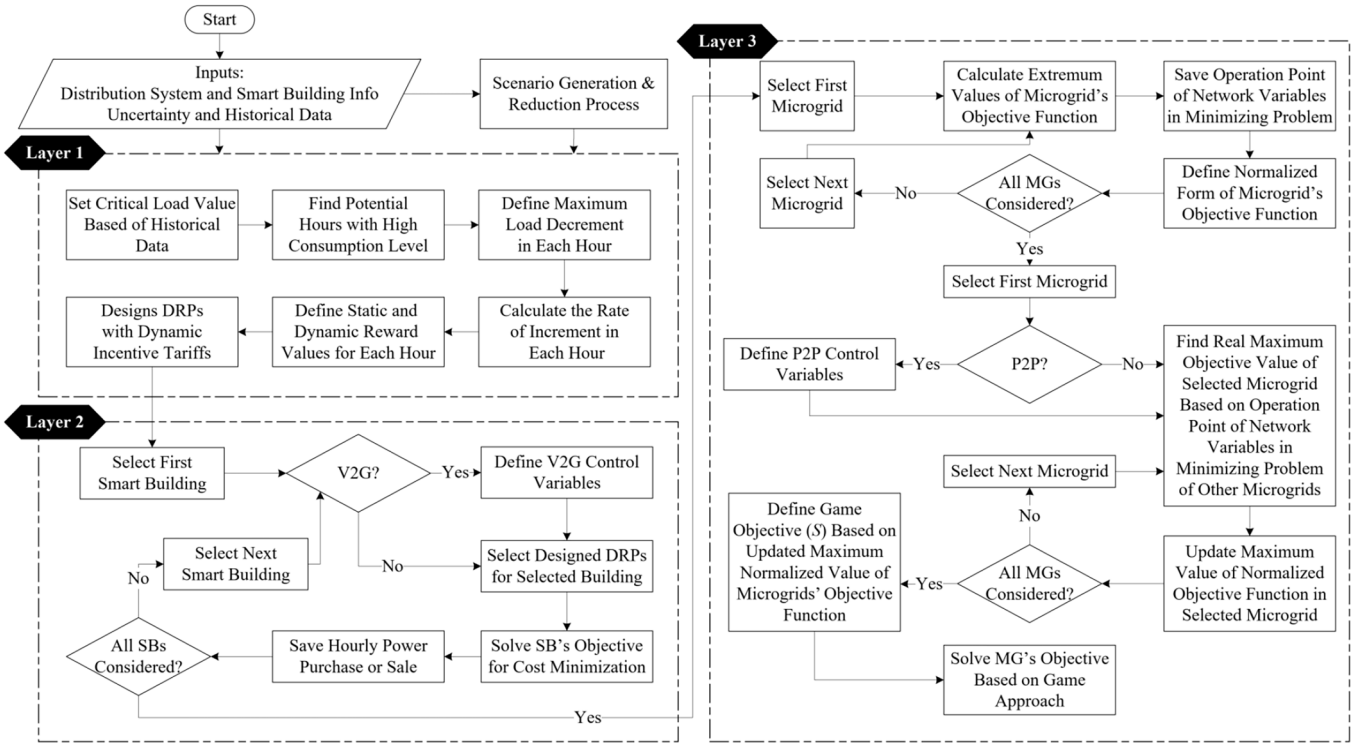

Fig. 1. Flowchart of the proposed three-layer DA scheduling strategy.

the residents' consumption behavior.

$$\widetilde{P}^{Load}_{b,t,sc} \geqslant P^{Avg,Load}_{b,sc} \Rightarrow \begin{cases} \widehat{P}^{L,DR-}_{b,t,sc} = \widetilde{P}^{Load}_{b,t,sc} - P^{Avg,Load}_{b,sc} \\ \pi^{L,DR-}_{b,t,sc} = \gamma^{R}\pi^{E}_{t}\left(1+\alpha^{R}e^{\varepsilon\left(\widehat{P}^{Load}_{b,t,sc}-P^{Avg,Load}_{b,sc}\right)}\right) \end{cases} \tag{1}$$

- **Layer 2**

In layer 2, SBs do their daily scheduling according to the DRPs received from the MG operator. The objective function of this layer is shown in Eq. (2) where the daily electricity bill of SBs is minimized. This function is calculated separately for each SB and includes the costs associated with purchasing power from the grid and using BES systems, and the benefits from providing V2G services and participating in DRPs.

$$\begin{aligned} C^{Building}_{b,sc} &= \sum_{t}\left(\pi^{E}_{t}P^{Building}_{b,t,sc}\right)\Delta t + \sum_{t}\sum_{e\in\Omega^{e}_{b}} C^{B}_{e,t,sc} \\ &-\sum_{t}\sum_{ev\in\Omega^{ev}_{b}}\left(\pi^{EV,Dch}_{t}P^{EV,Dis}_{ev,t,sc}\right)\Delta t - \sum_{t}\left(P^{L,DR-}_{b,t,sc}\pi^{L,DR-}_{b,t,sc}\right)\Delta t \end{aligned} \tag{2}$$

- **Layer 3**

In layer 3, the scheduling of MGs is done in a competitive environment through the implementation of a cooperative game, taking into account the requested programs of SBs. It should be stated that the risk-averse scheduling problem of each MG is modeled by Eqs. (3)-(12). In this regard, the objective function of MG m is minimized in Eq. (3). This equation illustrates that the daily costs of MG m include the operating costs associated with Gas Turbines (GTs) and BES systems, the net cost of exchanging power through grid or P2P, and the profit from selling power to SBs. (4) to (6) model P2P power sharing. Equations (4) and (5) respectively calculate the total purchase and total sales of each MG according to its links with other MGs. Equation (6) Ensures P2P balance.

$$\begin{aligned} C^{MG}_{m,sc} &= \sum_{g\in\Omega^{g}_{m}}\sum_{t} C^{G}_{g,t,sc} + \sum_{e\in\Omega^{e}_{m}}\sum_{t} C^{B}_{e,t,sc} + \sum_{l}\xi_{l,m}\sum_{t}\left(\pi^{E}_{t}P^{Line}_{l,t,sc}\right)\Delta t \\ &+\sum_{t}\left[\pi^{E}_{t}\left(P^{Buy,P2P}_{m,t,sc} - P^{Sell,P2P}_{m,t,sc}\right)\right]\Delta t - \sum_{b\in\Omega^{b}_{m}}\sum_{t}\left(\pi^{E}_{t}P^{Building}_{b,t,sc}\right)\Delta t \end{aligned} \tag{3}$$

$$P^{Buy,P2P}_{m,t,sc} = \sum_{n} P^{P2P}_{n,m,t,sc} \tag{4}$$

$$P^{Sell,P2P}_{m,t,sc} = \sum_{n} P^{P2P}_{m,n,t,sc} \tag{5}$$

$$P^{P2P}_{m,n,t,sc} = -P^{P2P}_{n,m,t,sc} \tag{6}$$

In (7)-(12), the IGDT-based RA strategy adopted to handle the scheduling risk of MGs is presented. In this regard, in (7) a separate zone is specified for the fluctuations of each stochastic parameter, i.e., load demand, wind and sun irradiance. φ_x refers to maximum deviation radius of each parameter. (8)-(12) model the RA strategy constraints. Note that in the proposed mechanism, underestimated load demand and overestimated wind speed and sun irradiance are taken into account since we want to secure MGs' scheduling against worst-case situation.

$$U\left(\varphi_x, x^{*}_{t}\right) = \left\{x_t : \frac{\left|x_t - x^{*}_{t}\right|}{x_t} \leqslant \varphi_x\right\} x \in \left\{v_{t,sc}, G_{t,sc}, P^{Demand}_{i,t,sc}, \widetilde{P}^{Load}_{b,t,sc}\right\} \tag{7}$$

$$\underset{x}{\widehat{\varphi}}\left(C^{MG}_{m,sc}\right) = \max\left\{\varphi^{RA}_{x} : \min C^{MG}_{m,sc} \leqslant C^{MG,RA}_{m}\right\} \tag{8}$$

$$C^{MG,RA}_{m} = (1+\delta)C^{MG,Det}_{m} \tag{9}$$

$$x_t = x^{*}_{t} \pm \varphi_x x^{*}_{t} \Rightarrow \begin{cases} x^{*}_{t} + \varphi_x x^{*}_{t}\ , & x \in \{\text{Load of MGs}\} \\ x^{*}_{t} - \varphi_x x^{*}_{t}\ , & x \in \{\text{Renewable Generation}\} \end{cases} \tag{10}$$

$$0 \leqslant \delta \leqslant 1 \tag{11}$$

$$\varphi_x \geqslant 0 \tag{12}$$

Table 2
Implementation of the proposed cooperative game.

Step 1:	**For** each MG, **m**: Set optimization type to Minimizing. Solve layer 3 for MG **m**. (Eqs. 3–12) **Put** the value in $f_m^{\min}$ Save optimal solution to x_m^* Set optimization type to Maximizing. Solve layer 3 for MG **m**. (Eqs. 3–12) **Put** the value in $f_m^{\max}$ **End**
Step 2:	**For** each MG, **m**: Normalize the objective function $f_m(x) \in \left[f_m^{\min}, f_m^{\max}\right]$ **End** $f_m(x) \xrightarrow{normalize} F_m(x)$
Step 3:	**For** each MG, **m**: $F_m^w = \max_{1 \leqslant n \leqslant M} F_m(x_n^*)$ **End**
Step 4:	Maximize S by solving following problem: $S = \prod_{m=1}^{M} \left[F_m^w - F_m(x)\right]$

Table 2 illustrates the implementation process of the proposed cooperative game. As per the pseudocode, the minimum and maximum values of the objective function of each MG are computed in step 1. To this end, Eqs. (3)-(12) are solved considering two different optimization types (minimizing / maximizing). In addition, in step 1, the optimal values obtained for the scheduling variables are stored in parameter x. In step 2, the normalize value of the objective function of each MG is calculated according to the minimum and maximum values obtained for it. In step 3, the maximum value of the objective function of each MG is identified. Lastly, in step 4, the optimal solution of MGs is calculated through the maximization of the S function. As can be seen, this function maximizes the product of the deviation of the optimal solution of MGs from their maximum value. Therefore, in this step, the final schedule of each MG is determined.

3.2. Distributed energy resources (DERs)

Several DERs has been modelled in this methodology, i.e., wind power, PV systems, gas turbines, BES systems, SBs and EVs [56]. Wind generators are described using (1a), where the actual generation $P_{w,t,sc}^{W}$ is modelled as a function of the wind speed $v_{t,sc}$ and the cut-in v_{ci}, cut-out v_{co}, rated v_r velocities and rated power $P_w^{W,\max}$. PV systems are modelled by (1b) considering η^{PV} as the efficiency of the panel, $G_{t,sc}$ as the sun irradiance at time period t, G^{STD} as the standard irradiance and, $P_{pv}^{PV,\max}$ as the rated PV panel power. Equations (1c) – (1e) model the behavior of gas turbines considering that their output power $P_{g,t,sc}^{G}$ has to be enclosed by lower $P_g^{G,min}$ and upper $P_g^{G,\max}$ bounds. Reactive power of gas turbines is modelled as a function of $P_{g,t,sc}^{G}$ using the parameter α_g^{max}, then, operation costs $C_{g,t,sc}^{G}$ are defined by (1e), where π_g^G is the generation price of the gas turbine.

$$P_{w,t,sc}^{W} \leqslant \begin{cases} 0\ , & v_{t,sc} < v_{ci} \text{ Or } v_{t,sc} \geqslant v_{co} \\ P_w^{W,\max}\left(\dfrac{v_{t,sc}^2 - v_{ci}^2}{v_r^2 - v_{ci}^2}\right)\ , & v_{ci} \leqslant v_{t,sc} < v_r \\ P_w^{W,\max}\ , & v_r \leqslant v_{t,sc} < v_{co} \end{cases} \tag{1a}$$

$$P_{pv,t,sc}^{PV} \leqslant \eta^{PV} \frac{G_{t,sc}}{G^{STD}} P^{PV,\max} \tag{1b}$$

$$P_g^{G,\min} \leqslant P_{g,t,sc}^{G} \leqslant P_g^{G,\max} \tag{1c}$$

$$-\alpha_g^{\max} P_{g,t,sc}^{G} \leqslant Q_{g,t,sc}^{G} \leqslant \alpha_g^{\max} P_{g,t,sc}^{G} \tag{1d}$$

$$C_{g,t,sc}^{G} = \pi_g^G P_{g,t,sc}^{G} \tag{1e}$$

3.3. Battery energy storage systems

BES systems are modelled as follows, discharging $P_{e,t,sc}^{B,Dis}$ and charging $P_{e,t,sc}^{B,Ch}$ are limited by maximum discharging $\gamma^{Dis,max}$ and charging $\gamma^{Ch,max}$ levels and the rated capacity Cap_e^B of the BES e by (2a) and (2b). Integer variables $I_{e,t,sc}^{B,Dis}$, $I_{e,t,sc}^{B,Ch}$ defined in (2c) avoid the simultaneous activation of charge and discharge of the BES system. State of Charge (SoC) is defined considering a per unit description in (2d) where charging and discharging power are modified by the efficiencies η^{Ch} and η^{Dis}. (2e) sets the SoC to $SOC^{B,Initial}$ at the start and end of operation. SoC is enclosed by an upper SoC^{max} and lower SoC^{min} limits in (2f) while the costs of their operation are described in (2g) considering π^B as the unitary cost per power unit delivered [57].

$$0 \leqslant P_{e,t,sc}^{B,Dis} \leqslant \gamma^{Dis,\max} Cap_e^B I_{e,t,sc}^{B,Dis} \tag{2a}$$

$$0 \leqslant P_{e,t,sc}^{B,Ch} \leqslant \gamma^{Ch,\max} Cap_e^B I_{e,t,sc}^{B,Ch} \tag{2b}$$

$$0 \leqslant I_{e,t,sc}^{B,Dis} + I_{e,t,sc}^{B,Ch} \leqslant 1 \tag{2c}$$

$$SOC_{e,t,sc}^{B} = SOC_{e,t-1,sc}^{B} + \frac{\eta^{Ch} P_{e,t,sc}^{B,Ch} - \frac{P_{e,t,sc}^{B,Dis}}{\eta^{Dis}}}{Cap_e^B} \Delta t \tag{2d}$$

$$SOC_{e,t=0,sc}^{B} = SOC_{e,t=24,sc}^{B} = SOC^{B,Initial} \tag{2e}$$

$$SOC^{\min} \leqslant SOC_{e,t,sc}^{B} \leqslant SOC^{\max} \tag{2f}$$

$$C_{e,t,sc}^{B} = \pi^B \left(P_{e,t,sc}^{B,Ch} + P_{e,t,sc}^{B,Dis}\right) \tag{2g}$$

3.4. Smart buildings and EV fleets

SBs effectively manages the Air Conditioning (AC) systems and Electric Water Heaters (EWHs) with regard to the DRP offered by the MG operator. In (3a), the maximum permissible load reduction through the DRP ($P_{b,t,sc}^{L,DR-}$) is determined. (3b) expresses that load reduction is possible only through AC ($P_{b,t,sc}^{AC}$) and EWH ($P_{b,t,sc}^{EWH}$). (3c) computes the final load demand of the SB after applying DRP.

$$0 \leqslant P_{b,t,sc}^{L,DR-} \leqslant \widehat{P}_{b,t,sc}^{L,DR-} \tag{3a}$$

$$P_{b,t,sc}^{L,DR-} = P_{b,t,sc}^{L,Desire} - P_{b,t,sc}^{EWH} - P_{b,t,sc}^{AC} \tag{3b}$$

$$P_{b,t,sc}^{Load} = \widetilde{P}_{b,t,sc}^{Load} - P_{b,t,sc}^{L,DR-} \tag{3c}$$

Temperature of the EWH of the building b is defined in (3d) as a function of the power $P_{b,t,sc}^{EWH}$ and the energy demand $Q_{b,t,sc}^{EWH}$. (3e) determines the water temperature inside the EWH tank at the beginning of operation. Temperature $\theta_{b,t,sc}^{W}$ is enclosed between $\theta_t^{W,min}$ and $\theta_t^{W,max}$ in (3f) and the energy demand $Q_{b,t,sc}^{EWH}$ is computed in (3g) considering the temperature of the cold water θ^{Cold}. Energy demand in EWH is met by (3h). (3i) models the EWH capacity limit. Losses of the tank are modelled through $Q_{b,t,sc}^{Loss}$ in (3j) considering the physical characteristics of the EWH, i.e., insulation thickness Δx and conductivity σ, the heat transfer coefficient h, the ambient temperature $\theta_{t,sc}^{Amb}$ and its surface $S_{surface}$.

$$\theta_{b,t,sc}^{W} = \theta_{b,t-1,sc}^{W} + \frac{P_{b,t,sc}^{EWH} \Delta t - Q_{b,t,sc}^{EWH} - Q_{b,t,sc}^{Loss}}{kpv_{b,t,sc}^{tank}} \tag{3d}$$

$$\theta_{b,t=0,sc}^{W} = \theta^{W,Initial} \tag{3e}$$

$$\theta_t^{W,\min} \leqslant \theta_{b,t,sc}^{W} \leqslant \theta_t^{W,\max} \tag{3f}$$

$$Q_{b,t,sc}^{EWH} = kpv_{b,t,sc}^{tank} \left(\theta_{b,t,sc}^{W} - \theta^{Cold}\right) \tag{3g}$$

$$P_{b,t,sc}^{EWH} \Delta t \geqslant Q_{b,t,sc}^{EWH} \tag{3h}$$

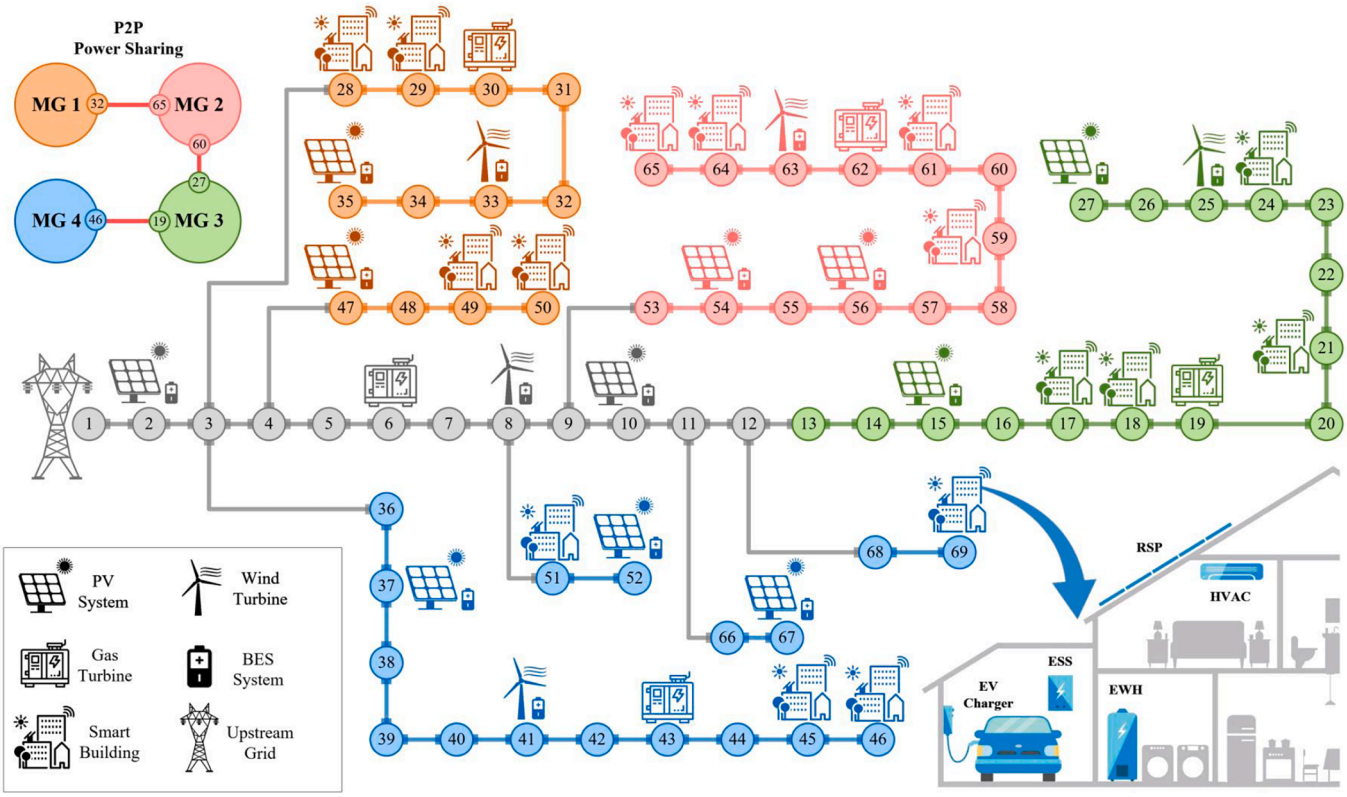

Fig. 2. Architecture of the case study based on a 69-node DS with four MGs.

$$0 \leqslant P^{EWH}_{b,t,sc} \leqslant P^{EWH,\max}_{b} \tag{3i}$$

$$Q^{Loss}_{b,t,sc} = \frac{\theta^{W}_{b,t,sc} - \theta^{Amb}_{t,sc}}{\frac{\Delta x}{\sigma} + \frac{1}{h}} S_{surface} \tag{3j}$$

Temperature of the building $\theta^{B}_{b,t,sc}$ is updated in (3k) considering the thermal constant of the building α^{B}, the ambient temperature $\theta^{Amb}_{t,sc}$ and the AC power $P^{AC}_{b,t,sc}$ which is limited by (3n). (3l) determines the temperature of the building at the beginning of operation. This temperature must be enclosed between $\theta^{B,min}_{t}$ and $\theta^{B,max}_{t}$ in (3m). The TC index of SB is computed by (3o) according to the temperature of the building and water temperature. Note that the Big-M technique has been used to linearize the non-linear term caused by the absolute value. (3p) is included in the formulation to prevent TC index from going out of the allowed range.

$$\theta^{B}_{b,t,sc} = (1-\alpha^{B})\theta^{B}_{b,t-1,sc} + \alpha^{B}\theta^{Amb}_{t,sc} + \alpha^{AC} P^{AC}_{b,t,sc} \Delta t \tag{3k}$$

$$\theta^{B}_{b,t=0,sc} = \theta^{B,Initial} \tag{3l}$$

$$\theta^{B,\min}_{t} \leqslant \theta^{B}_{b,t,sc} \leqslant \theta^{B,\max}_{t} \tag{3m}$$

$$0 \leqslant P^{AC}_{b,t,sc} \leqslant P^{AC,\max}_{b} \tag{3n}$$

$$TC_{b,sc} = \frac{\sum_t \left[1 - \tau \left| \theta^{B,Desire} - \theta^{B}_{b,t,sc} \right|\right] + \sum_t \left[1 - \tau \left| \theta^{W,Desire} - \theta^{W}_{b,t,sc} \right|\right]}{48} \times 100 \tag{3o}$$

$$TC_{b,sc} \geqslant TC^{\min} \tag{3p}$$

EVs operation is defined considering a mixed integer model, using binary variables $I^{EV,Ch}_{ev,t,sc}$, $I^{EV,Dis}_{ev,t,sc}$ associated to charging and discharging strategies. Charging and discharging operations of the EV can be only activated between arrival T^{a}_{b} and departure T^{d}_{b} times in (3q) and (3r). (3s) does not allow the simultaneous activation of the binary variables of charge and discharge. SoC is updated in (3t)–(3v) and must be enclosed between SoC^{min} and SoC^{max} in (3w).

$$\begin{cases} 0 \leqslant P^{EV,Ch}_{ev,t,sc} \leqslant \gamma^{Ch,\max} Cap^{EV}_{ev} I^{EV,Ch}_{ev,t,sc} \\ 0 \leqslant P^{EV,Dis}_{ev,t,sc} \leqslant \gamma^{Dis,\max} Cap^{EV}_{ev} I^{EV,Dis}_{ev,t,sc} \end{cases} t \in [T^{a}_{b}, T^{d}_{b}) \tag{3q}$$

$$\begin{cases} P^{EV,Ch}_{ev,t,sc} = 0 \\ P^{EV,Dis}_{ev,t,sc} = 0 \end{cases} t \notin [T^{a}_{b}, T^{d}_{b}) \tag{3r}$$

$$0 \leqslant I^{EV,Ch}_{ev,t,sc} + I^{EV,Dis}_{ev,t,sc} \leqslant 1 \tag{3s}$$

$$SOC^{EV}_{ev,t,sc} = SOC^{EV}_{ev,t-1,sc} + \frac{\eta^{Ch} P^{EV,Ch}_{ev,t,sc} - \frac{P^{EV,Dis}_{ev,t,sc}}{\eta^{Dis}}}{Cap^{EV}_{ev}} \Delta t \tag{3t}$$

$$SOC^{EV}_{ev,t=T^{a},sc} = SOC^{EV,Initial}_{ev} \tag{3u}$$

$$SOC^{EV}_{ev,t=T^{d},sc} = SOC^{EV,Final}_{ev} \tag{3v}$$

$$SOC^{\min} \leqslant SOC^{EV}_{ev,t,sc} \leqslant SOC^{\max} \tag{3w}$$

The overall power demand of the SB $P^{Building}_{b,t,sc}$ is the sum of the load demand $P^{Load}_{b,t,sc}$, BES systems, EVs and PV solar $P^{PV}_{pv,t,sc}$.

$$P^{Building}_{b,t,sc} = P^{Load}_{b,t,sc} + \sum_{e \in \Omega^{e}_{b}} \left(P^{B,Ch}_{e,t,sc} - P^{B,Dis}_{e,t,sc} \right) + \sum_{ev \in \Omega^{ev}_{b}} \left(P^{EV,Ch}_{ev,t,sc} - P^{EV,Dis}_{ev,t,sc} \right) - \sum_{pv \in \Omega^{pv}_{b}} P^{PV}_{pv,t,sc} \tag{3x}$$

Table 3
Structure of the different scenarios for the 69-bus system case study.

Case	RA Strategy	P2P Power Transaction	DRP Modelling		V2G Services
			Static-Tariffs	Dynamic-Tariffs	
C1	x	x	x	x	x
C2	✓	x	x	x	x
C3	✓	✓	x	x	x
C4	✓	✓	✓	x	x
C5	✓	✓	x	✓	x
C6	✓	✓	x	✓	✓

3.5. Power flow

We consider a quadratic representation of the power flow equations which considers both the active and reactive power flow of the microgrids [38]. Active and reactive power flows are computed in (4a) and (4b), while power losses for line l are computed according to (4c) based on the resistance R_l of the branch. Thermal branch limits are computed in (4d) and voltage magnitude and phase angle are computed in (4e) and (4f), respectively. Note that the quadratic terms $\left(P^{Line}_{l,t,sc}\right)^2$ and $\left(Q^{Line}_{l,t,sc}\right)^2$ in Eqs. (4c) and (4d) are linearized using the piecewise linearization technique [38]. Equations (4g) and (4h) defines the active and reactive node balances in the grid respectively, based on the power demands of the DERs.

$$P^{Line}_{l,t,sc} = G_l\left(V_{i,t,sc} - V_{j,t,sc}\right) + B_l\left(\theta_{i,t,sc} - \theta_{j,t,sc}\right) \tag{4a}$$

$$Q^{Line}_{l,t,sc} = B_l\left(V_{i,t,sc} - V_{j,t,sc}\right) - G_l\left(\theta_{i,t,sc} - \theta_{j,t,sc}\right) \tag{4b}$$

$$P^{Loss}_{l,t,sc} = R_l\left[\left(P^{Line}_{l,t,sc}\right)^2 + \left(Q^{Line}_{l,t,sc}\right)^2\right] \tag{4c}$$

$$0 \leqslant \left(P^{Line}_{l,t,sc}\right)^2 + \left(Q^{Line}_{l,t,sc}\right)^2 \leqslant \left(S^{Line,\max}_{l}\right)^2 \tag{4d}$$

$$V^{\min} \leqslant V_{i,t,sc} \leqslant V^{\max} \tag{4e}$$

$$\theta^{\min} \leqslant \theta_{i,t,sc} \leqslant \theta^{\max} \tag{4f}$$

$$P^{Grid}_{t,sc}\Big|_{i=1} + \sum_{g\in\Omega^g_i} P^{G}_{g,t,sc} + \sum_{pv\in\Omega^{pv}_i} P^{PV}_{pv,t,sc} + \sum_{w\in\Omega^{w}_i} P^{W}_{w,t,sc} + \sum_{e\in\Omega^{e}_i}\left(P^{B,Dis}_{e,t,sc} - P^{B,Ch}_{e,t,sc}\right) = \sum_{l}\left(\xi_{l,i}P^{Line}_{l,t,sc} + \frac{P^{Loss}_{l,t,sc}}{2}\right) + \sum_{b\in\Omega^b_i} P^{Building}_{b,t,sc} + P^{Demand}_{i,t,sc} \tag{4g}$$

$$Q^{Grid}_{t,sc}\Big|_{i=1} + \sum_{g\in\Delta^g_i} Q^{G}_{g,t,s} = \sum_{l\in\Delta^l_i}\xi_{l,i}Q^{Line}_{l,t,s} + \sum_{b\in\Omega^b_i}\tan(\varphi_i)P^{Building}_{b,t,sc} + Q^{Demand}_{i,t,sc} \tag{4h}$$

4. Simulation results and discussions

4.1. Studied system

In this section, a case study that builds on the 69-node DS of the Fig. 2 is presented. Four MGs are depicted, MG1 in orange, MG2 in pink, MG3 in green and MG4 in blue. MG1 has 12 nodes where 1 WTs with BES systems, 2 PV systems with BES systems, and 1 GTs are connected. MG2 has 13 nodes where 1 GTs, 2 PV system with BES system and 1 wt with BES system are connected. MG3 has 15 nodes where 1 GTs and 1 WTs with BES system and 2 PV systems with BES systems are coupled. MG4 is composed of 17 nodes, 1 GTs and 1 WTs with BES system and 3 PV systems with BES systems. Lastly, the gray busses belong to DS. Note that the total load of the case study at peak hour is 3802.1 kW.

Table 4
Information on equipment of DS and MGs.

GTs					
No.	**Node**	**Generation Capacity (kW)**	**Marginal Cost ($/kW)**	**Reactive Capacity Level (%)**	**Owner**
1	6	300	0.07	50	DS
2	19	350	0.09	50	MG 3
3	30	500	0.08	50	MG 1
4	43	300	0.09	50	MG 4
5	62	600	0.08	50	MG 2
Renewable Generations					
No.	**Node**	**Generation Capacity (kW)**	**Type**	**Owner**	
1	8	300	WT	DS	
2	25	700	WT	MG 3	
3	33	500	WT	MG 1	
4	41	300	WT	MG 4	
5	63	600	WT	MG 2	
6	2	150	PV System	DS	
7	10	100	PV System	DS	
8	15	200	PV System	MG 3	
9	27	300	PV System	MG 3	
10	35	250	PV System	MG 1	
11	37	100	PV System	MG 1	
12	47	300	PV System	MG 4	
13	52	100	PV System	MG 4	
14	54	450	PV System	MG 4	
15	56	450	PV System	MG 2	
16	67	150	PV System	MG 2	

Table 5
Information on location and components of SBs.

No.	Node	PV Capacity (kW)	NoC	Number of EVs	Owner
1	17	20	60	42	MG 3
2	18	20	60	42	MG 3
3	21	40	114	80	MG 3
4	24	20	28	20	MG 3
5	28	20	26	18	MG 1
6	29	20	26	18	MG 2
7	45	20	39	27	MG 4
8	46	20	39	27	MG 4
9	49	100	385	270	MG 1
10	50	100	385	270	MG 1
11	51	20	41	29	MG 4
12	59	40	100	70	MG 2
13	61	60	177	124	MG 2
14	64	60	227	159	MG 2
15	65	20	59	41	MG 2
16	69	20	28	20	MG 4

Table 6
Initialization of simulation parameters [38].

Parameters	$\theta^{W,Initial}$	$\theta^{B,Initial}$	θ^{Cold}	$\theta^{\min}/\theta^{\max}$	η^{Ch}/η^{Dis}
Values (Unit)	45 (C°)	24 (C°)	15 (C°)	$-\pi/\pi$ (rad)	95 (%)
Parameters	α^{AC}	α^{B}	α^{R}	β	η^{PV}
Values (Unit)	11	0.9	0.5	95 (%)	98 (%)
Parameters	T^a/T^d	$v_{ci}/v_r/v_{co}$	G^{STC}	ω	γ^R
Values (Unit)	17:00/ 8:00 (h)	4/10/17 (m/s)	1000 (W/m^2)	0.5	0.04 ($/kWh)

4.2. Description of the simulations of the case study

The validity and effectiveness of the introduced three-layer cooperative game-theoretic based strategy is checked by implementing it on the cases listed in Table 3. Different simulations are performed, activating different characteristics of the proposed three-layer strategy, i.e.,

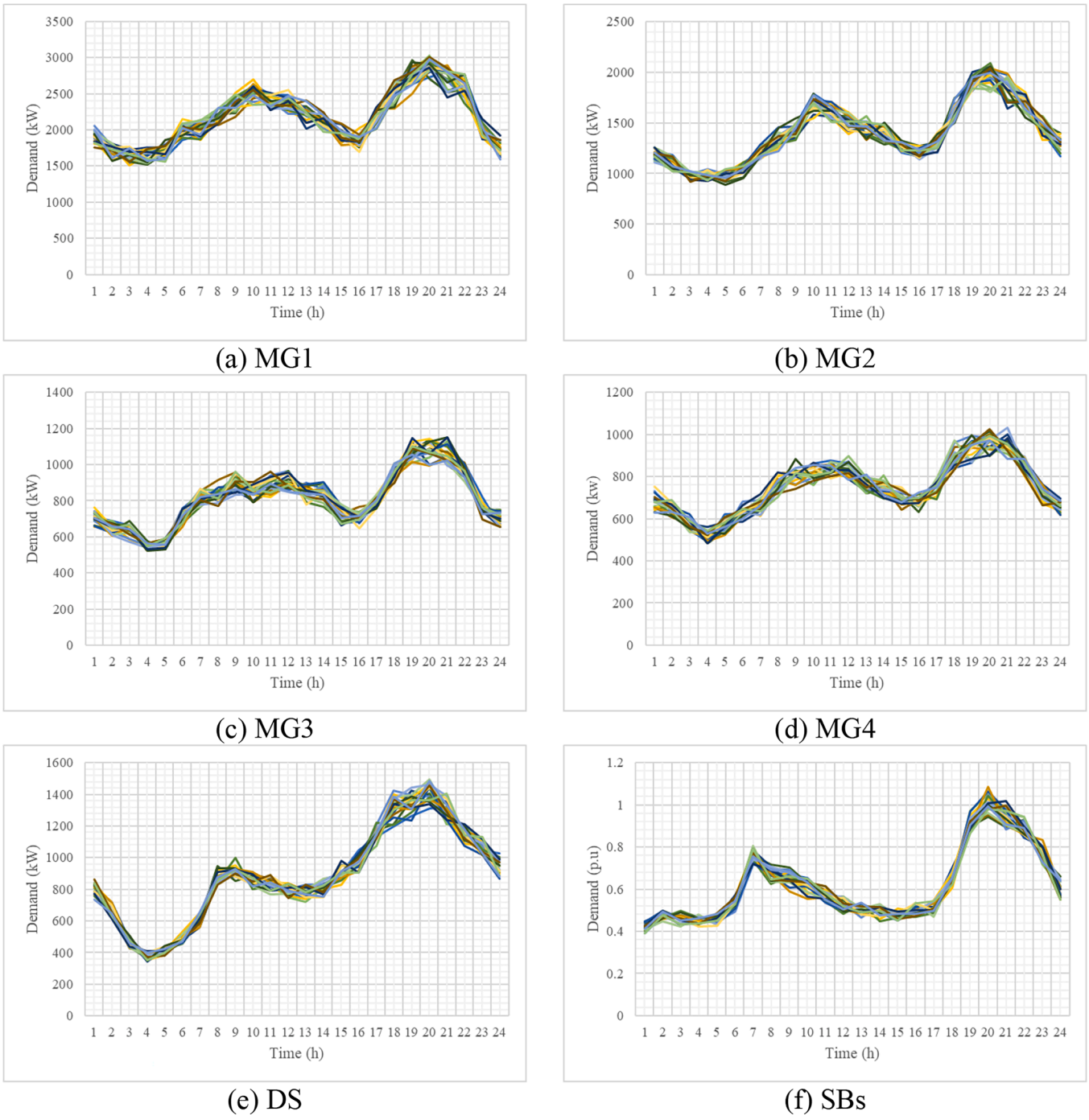

Fig. 3. The hourly load demand scenarios of SBs, MGs and DS.

RA strategy, P2P transactions, static- and dynamic-tariff DRPs, and V2G services. Table 4 tabulates information on equipment of DS and MGs, whereas Table 5 provides information on SBs location and their components. In Table 6, the simulation parameters are set. The load demand scenarios of SBs, MGs and DS are shown in Fig. 3a-3f. In Fig. 4a, the ambient temperature is depicted. Fig. 4b displays the hourly curve of SB' hot water demand. Fig. 5a and 5b depict wind and radiation scenarios. Ultimately, an electricity price curve with real-time format is presented in Fig. 6, according to which SBs and MGs do their DA scheduling.

4.3. Simulations results of C1 and C2

Tables 7 and 8 respectively tabulate the numerical outputs from simulating C1 and C2, where the proposed strategy is simulated in deterministic and RA modes, respectively. The analysis of the numerical outputs of Tables 7 and 8 indicates that the application of the RA strategy in C2 has increased the costs of MG1 to MG4 by 8.69%, 16.24%, 16.56% and 23.72%, respectively, compared to C1 (deterministic mode). By analyzing the numbers presented in Tables 7 and 8, it can be seen that applying the RA strategy has increased the costs of power exchange and equipment operation in C2 over C1.

In Fig. 7a-7d, safe regions created using RA strategy for MGs load fluctuations are shown, by analyzing them, it can be understood that the created safe regions are able to cover all scenarios. Similarly, Fig. 8a and 8b show the safe regions created for wind and radiation fluctuations, respectively, and their analysis also confirms that all scenarios are

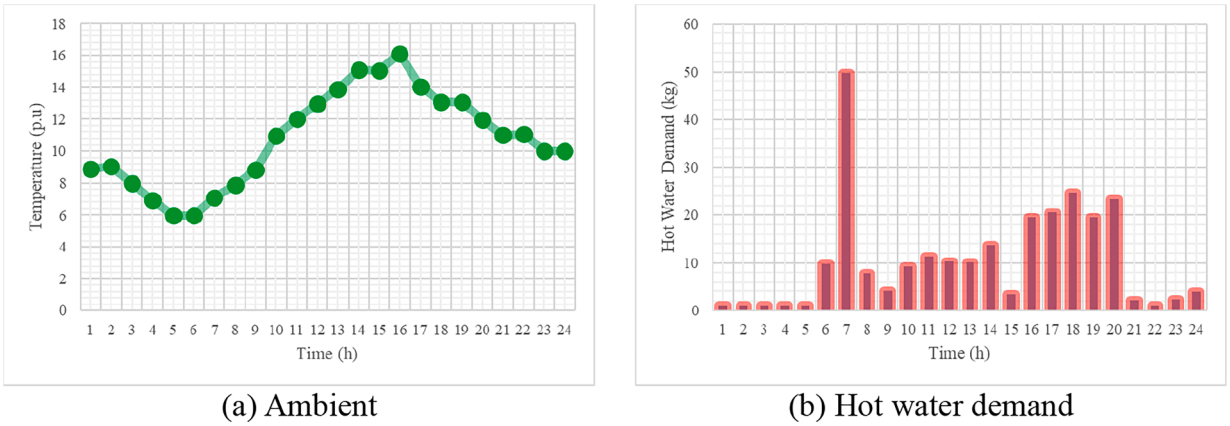

Fig. 4. Ambient temperature and occupant's desired temperature for indoor space.

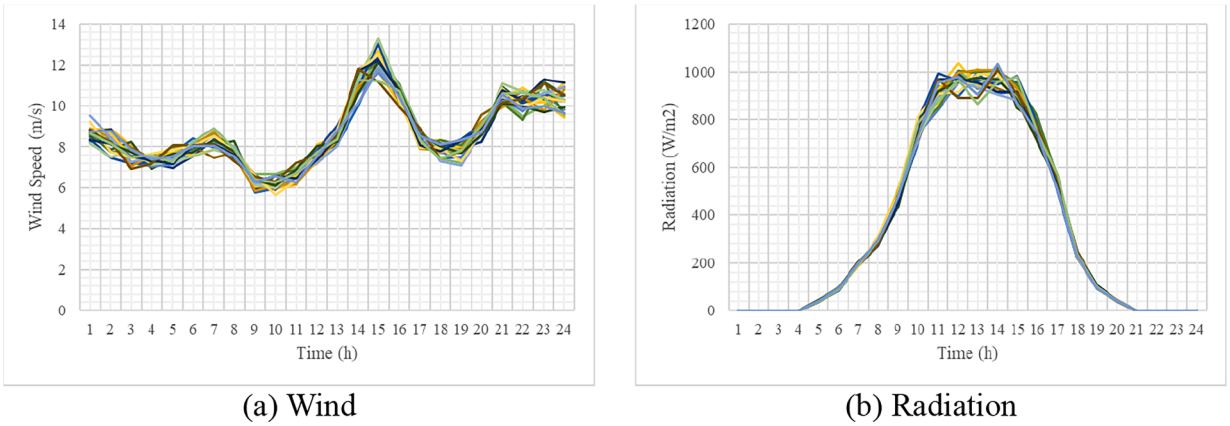

Fig. 5. Wind and radiation scenarios.

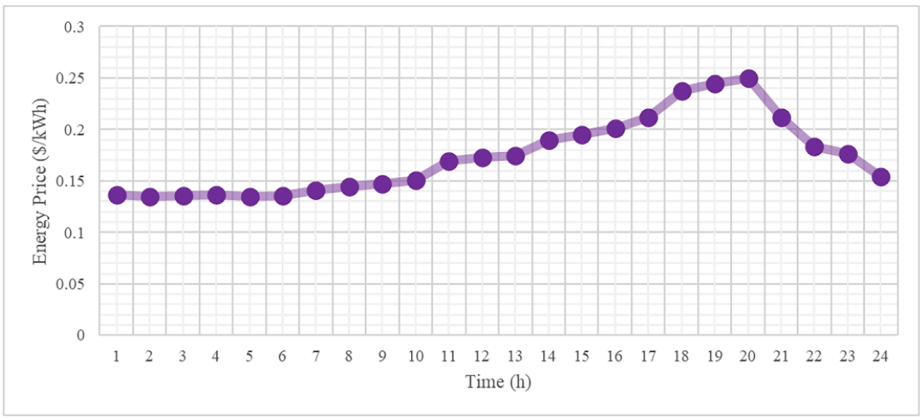

Fig. 6. The hourly electricity price curve.

Table 7
Costs results for the simulation C1. Results are in $.

Actors	GTs ($)	BES Systems ($)	Transactions ($)		DRPs ($)	Total ($)	Profit from Selling Power to Customers ($)	
			Grid	P2P			SBs	RBs
MG1	715.03	13.20	3,514.68	0.00	0.00	4,242.91	6,491.02	1,164.92
MG2	894.30	21.32	154.39	0.00	0.00	1,070.00	4,457.88	797.28
MG3	773.09	18.18	−581.78	0.00	0.00	209.49	1,957.69	1,154.40
MG4	419.06	8.20	568.86	0.00	0.00	996.12	1,152.41	1,738.30
DS	302.40	14.62	2,230.36	0.00	0.00	2,547.38	0.00	3,910.75
Sum	3,103.88	75.52	5,886.51	0.00	0.00	9,065.90	14,059.00	8,765.64

Table 8
Costs results for the simulation C2. Results are in $.

Actors	GTs ($)	BES Systems ($)	Transactions ($)		DRPs ($)	Total ($)	Profit from Selling Power to Customers ($)	
			Grid	P2P			SBs	RBs
MG1	844.98	13.19	3,753.28	0.00	0.00	4,611.45	6,830.91	1,281.41
MG2	942.22	23.03	278.50	0.00	0.00	1243.76	4,659.09	877.00
MG3	790.88	17.61	−564.30	0.00	0.00	244.18	1,987.04	1,269.84
MG4	544.51	8.20	679.65	0.00	0.00	1,232.37	1,234.55	1,912.13
DS	396.20	12.71	2,677.10	0.00	0.00	3,086.02	0.00	4,301.83
Sum	3,518.79	74.75	6,824.23	0.00	0.00	10,417.77	14,711.59	9,642.21

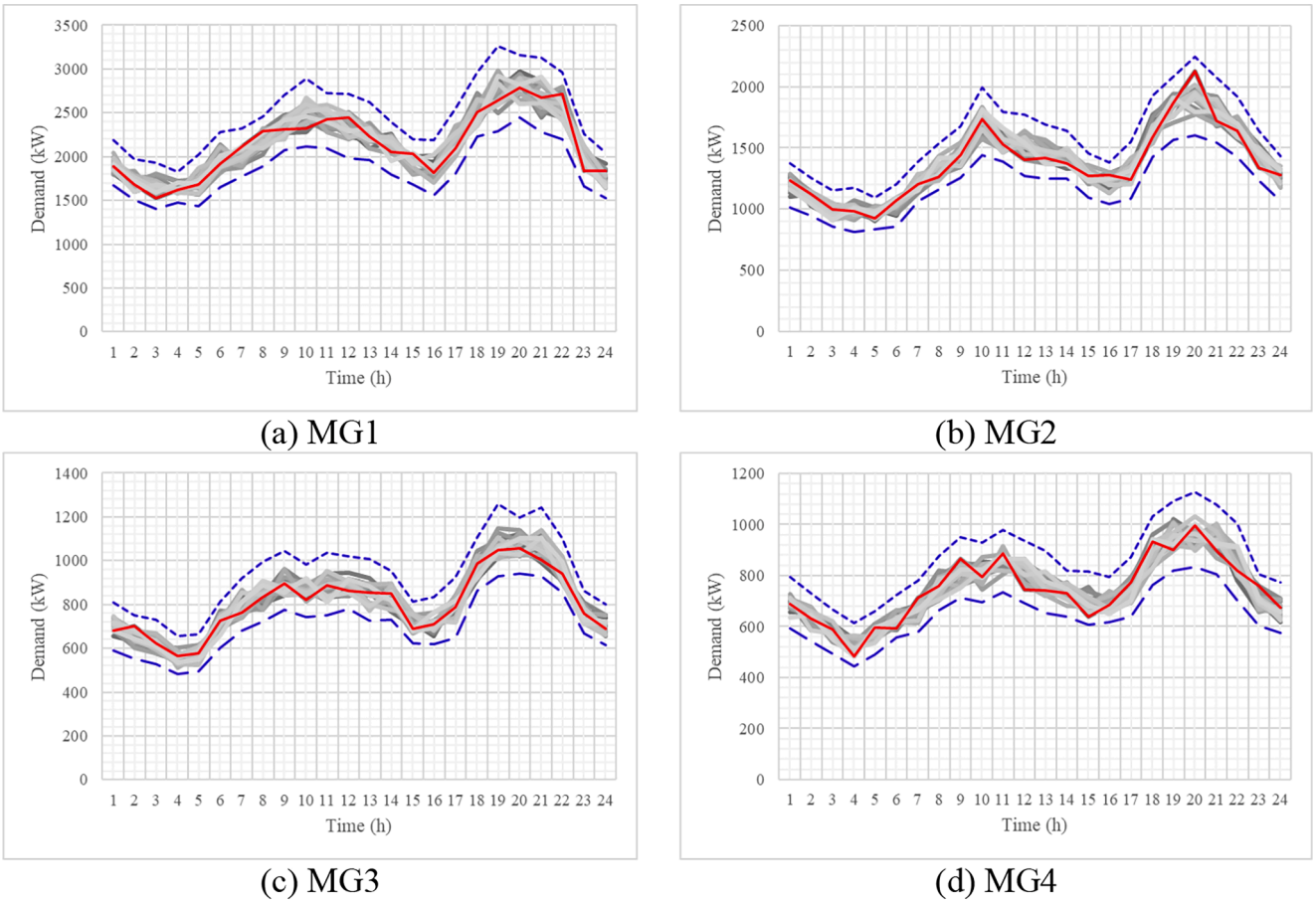

Fig. 7. The safe region created for MGs' load fluctuations: C1 & C2.

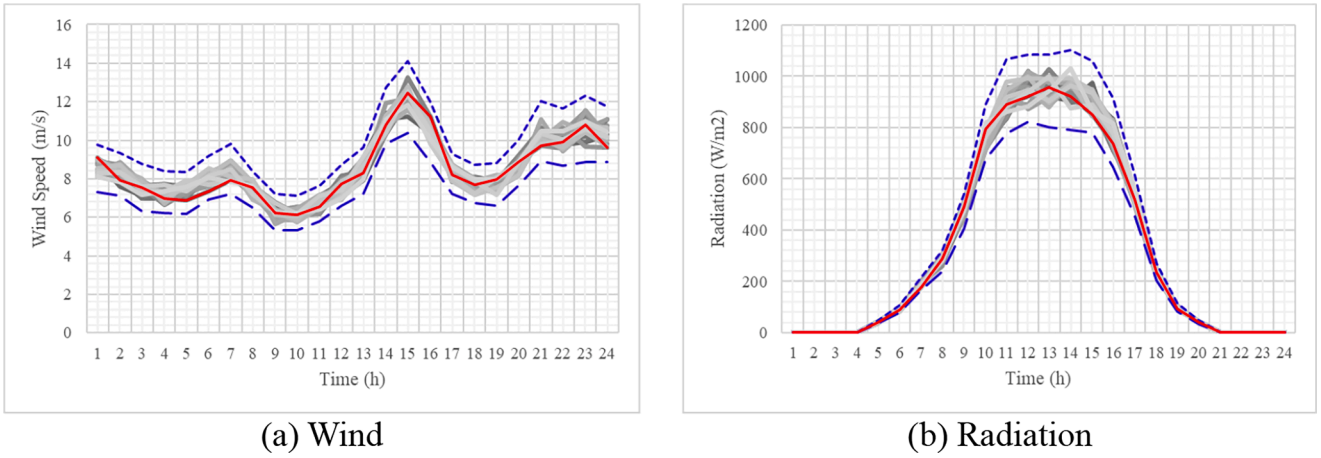

Fig. 8. The safe region created for wind and radiation fluctuations: C1 & C2.

Table 9
Costs results for the simulation C3.

Actors	GTs ($)	BES Systems ($)	Transactions ($)		DRPs ($)	Total ($)	Profit from Selling Power to Customers ($)	
			Grid	P2P			SBs	RBs
MG1	894.95	12.90	3,753.28	−591.54	0.00	4,069.59	6,830.91	1,281.41
MG2	696.83	20.51	78.50	250.61	0.00	1,046.45	4,659.09	877.00
MG3	832.38	18.32	−403.08	−220.25	0.00	227.36	1,987.04	1,269.84
MG4	533.22	8.20	553.02	74.18	0.00	1,168.62	1,234.55	1,912.13
DS	392.82	13.12	2,669.66	0.00	0.00	3,075.61	0.00	4,301.83
Sum	3,350.20	73.06	6,651.38	−487.00	0.00	9,587.63	14,711.59	9,642.21

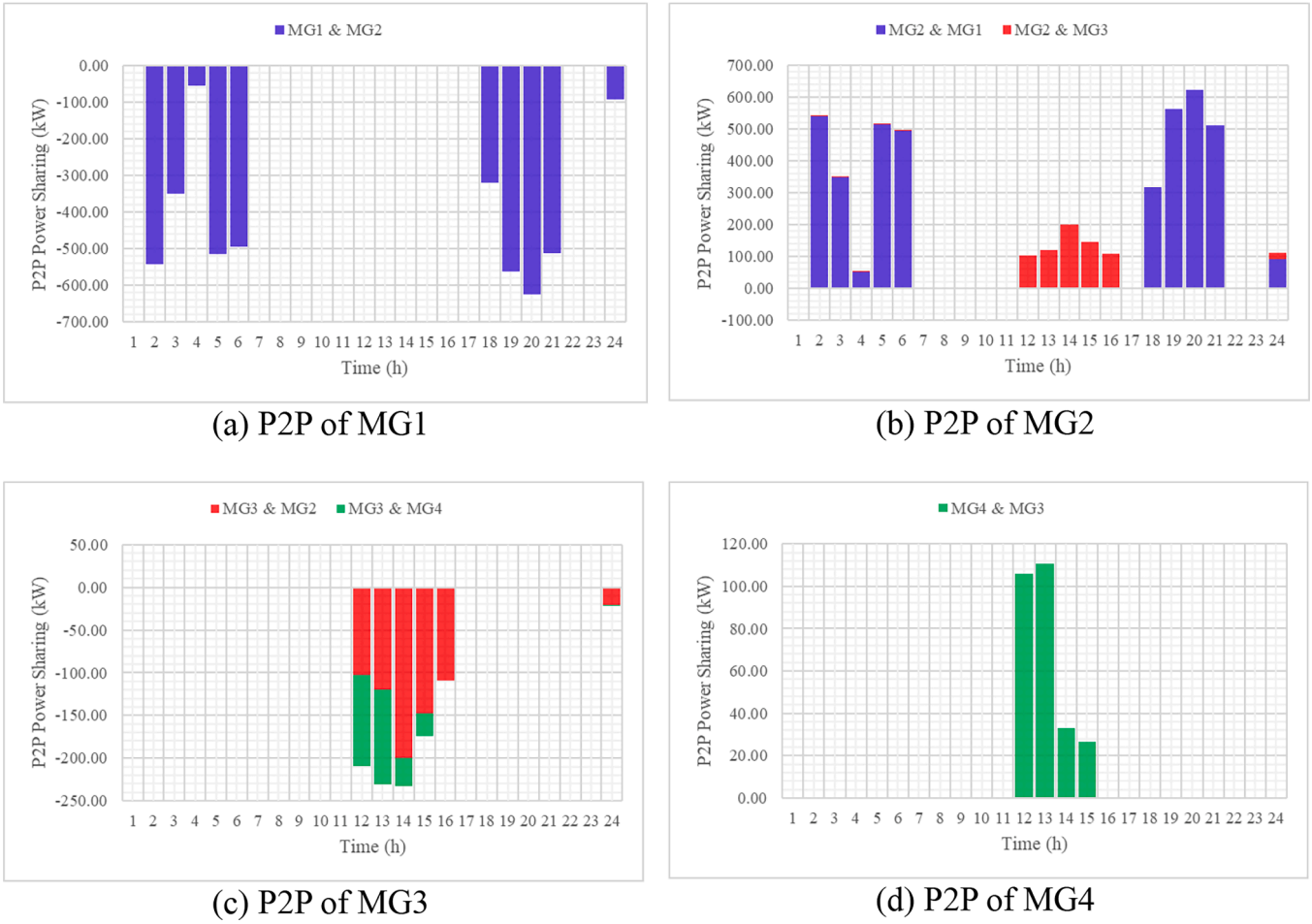

Fig. 9. Powers exchanged by P2P infrastructure: C3.

within safe regions. The upper and lower bounds of the safe region are shown in blue dashed lines, while the scenarios and the deterministic curve are shown in gray and red, respectively.

Note that RA strategy is not applied in C1 and therefore there is no safe region for the fluctuations of load, wind and sun radiation parameters. In other words, in C1, operation is applicable only for the deterministic curves of the load, radiation and wind, and otherwise the energy balance of the system will face a mismatch. Overall, it can be concluded from the simulation outputs of C1 and C2 that the application of the RA strategy, despite the relative increase in costs, has led to the creation of a safe region for MGs, which guarantees the stability of operation against the fluctuations of uncertain parameters.

4.4. Simulations results of C3

The proposed three-layer strategy in C3 is simulated by considering the P2P power transaction option among MGs. The numerical outputs obtained from the simulation of this case are presented in Table 9, where the numbers represent a reduction of 11.75%, 15.86%, 6.89% and 5.17% respectively in the daily costs of MG1 to MG4 over C2. The price of P2P power transaction is assumed to be equal to 80% of the hourly power transaction with the grid, since in the P2P structure, MGs do not use network facilities or intermediaries.

Fig. 9a-9d display the power transacted among MGs by the P2P infrastructures, where it is evident that MGs 2 and 4 are buyers, while MGs 1 and 3 are sellers. The analysis of these figures reveals that MGs 1 and 3 have been able to sell their excess production capacity to MGs 2 and 4 through P2P infrastructures. Fig. 10a-10d illustrate the production level of GTs in MGs 1 to 4, and their analysis clear that the production levels of GTs placed in MGs 1 and 3 during noon in C3 have increased compared to C2 as MGs in C3 have more links for power exchange due to the existence of P2P infrastructures. The reason for the reduction of the operating point of GTs during noon was the high operating point of PV systems during this period.

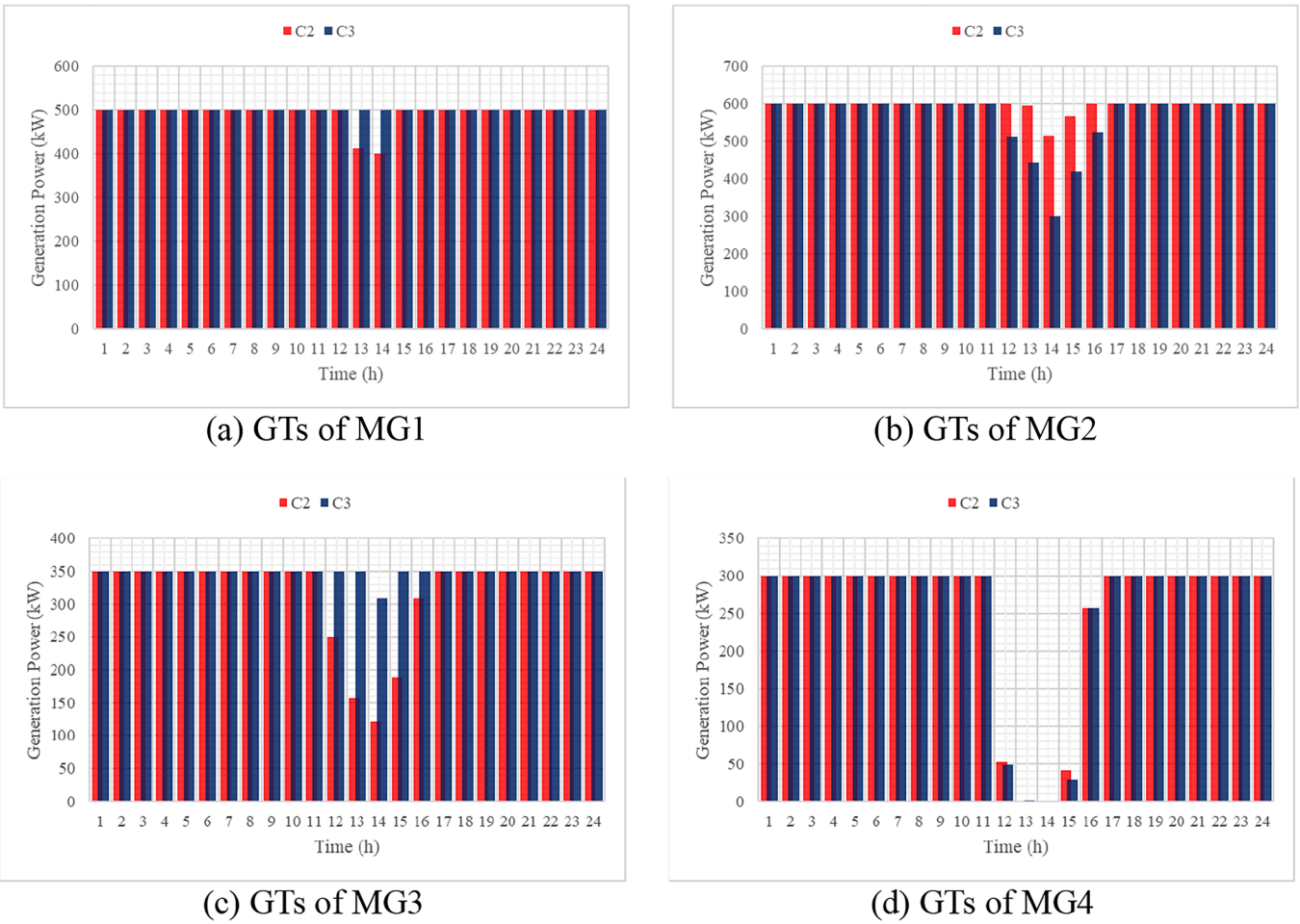

Fig. 10. GTs production level in MGs: C2 & C3.

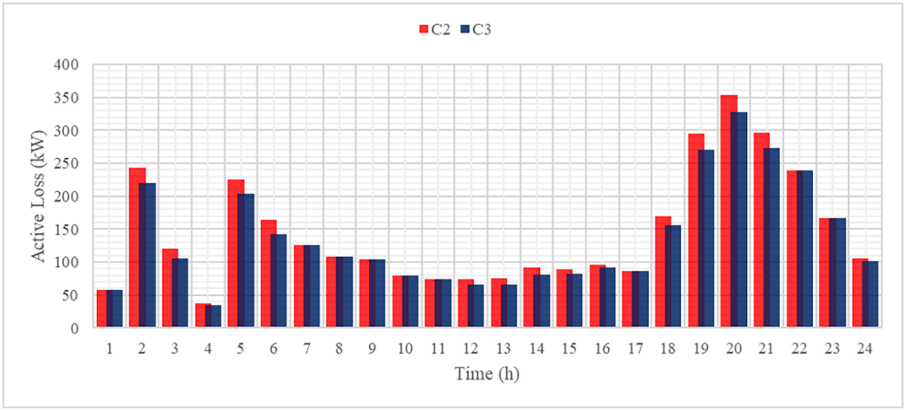

Fig. 11. Hourly power losses of the entire system: C2 & C3.

One of the advantages of P2P power sharing is reducing the dependence of MGs on the distribution system. It should be noted that the percentage of dependence of MGs on the distribution system is equal to the percentage of their load that is provided through purchase from the distribution system. Fig. 9a-9d clearly indicate that MGs 2 and 4 have been able to supply a significant part of their load in C3 by P2P exchange instead of exchange with the distribution grid, thereby reducing their dependence on the grid. In general, MGs prefer to buy the required power of their service area through P2P infrastructure instead of the grid as the exchange price of P2P is cheaper. Although an MG can meet its demands through the P2P infrastructure only during the hours when the MGs linked to it have excess power for sale.

Fig. 11 compares the hourly losses of the entire system in C2 and C3. As per this figure, power losses have decreased in all the hours when the power exchange has been done by P2P infrastructures, which is due to the reduction of the length of the power transmission path in the P2P structure. It should be mentioned that this reduction in losses leads to a significant increase in energy efficiency and also a reduction in operating costs in the system.

Table 10
Costs results for the simulation C4.

Actors	GTs ($)	BES Systems ($)	Transactions ($)		DRPs ($)	Total ($)	Profit from Selling Power to Customers ($)	
			Grid	P2P			SBs	RBs
MG1	894.95	13.20	3,549.19	−591.54	48.14	3,913.94	6,588.02	1,281.41
MG2	696.83	18.92	23.04	250.61	32.88	1,022.29	4,493.18	877.00
MG3	832.38	17.04	−480.89	−220.25	14.03	162.31	1,916.24	1,269.84
MG4	533.22	8.20	508.33	74.18	8.79	1,132.72	1,190.22	1,912.13
DS	392.82	13.34	2,485.16	0.00	0.00	2,891.32	0.00	4,301.83
Sum	3,350.20	70.71	6,084.83	−487.00	103.84	9,122.57	14,187.66	9,642.21

Table 11
Costs results for the simulation C5.

Actors	GTs ($)	BES Systems ($)	Transactions ($)		DRPs ($)	Total ($)	Profit from Selling Power to Customers ($)	
			Grid	P2P			SBs	RBs
MG1	894.95	13.19	3,345.10	−709.65	200.29	3743.89	6,532.17	1,281.41
MG2	696.83	18.92	−132.42	258.85	100.59	942.77	4,454.93	877.00
MG3	832.38	16.07	−558.69	−203.73	27.08	113.11	1,899.79	1,269.84
MG4	533.22	8.20	463.64	54.53	14.48	1,074.06	1,179.80	1,912.13
DS	392.82	14.02	2,300.65	0.00	0.00	2,707.49	0.00	4,301.83
Sum	3,350.20	70.41	5,418.28	−600.00	342.44	8,581.32	14,066.69	9,642.21

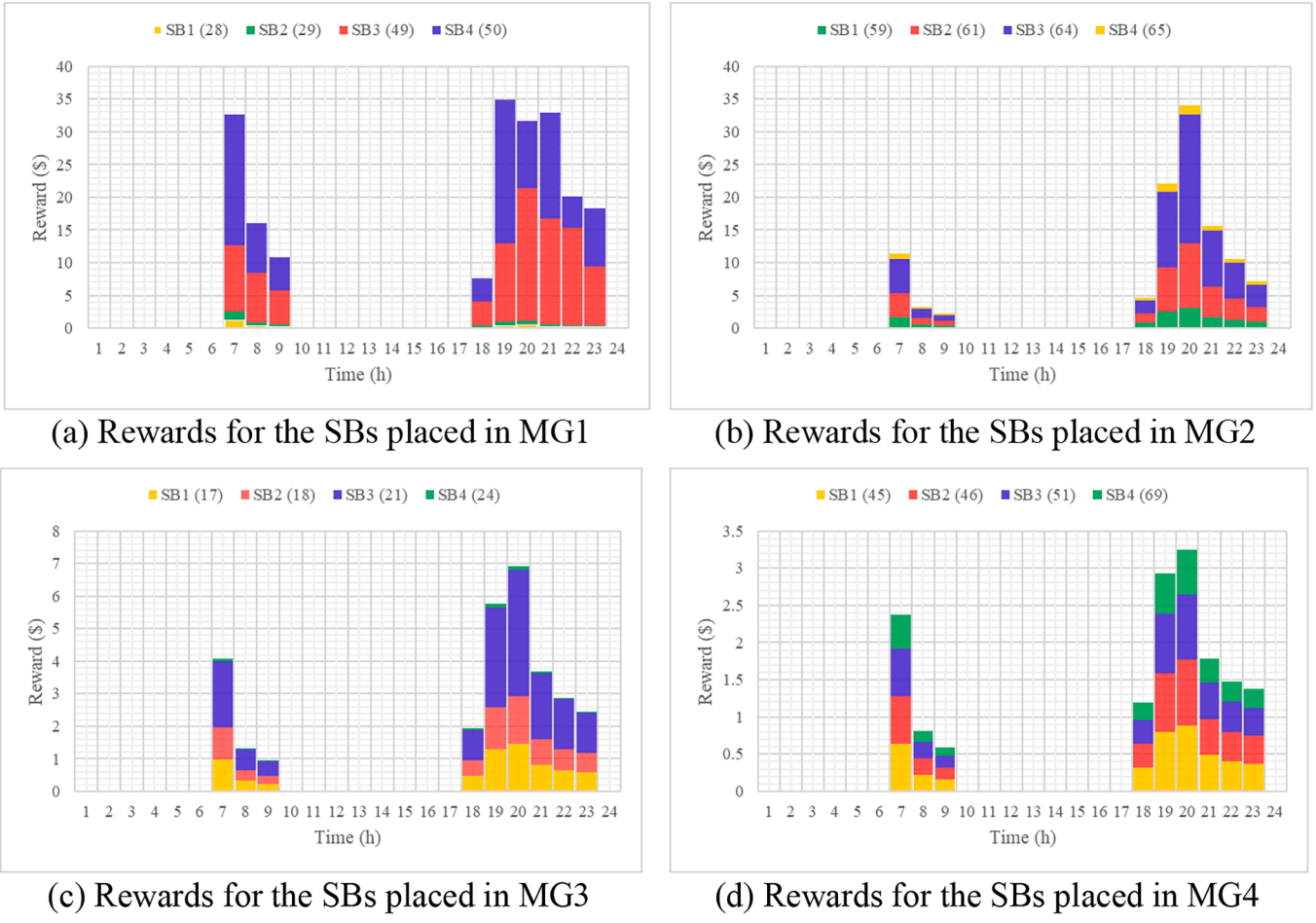

Fig. 12. Hourly rewards for the dynamic-tariff DRP: C5.

4.5. Simulations results of C4 and C5

In C4 and C5, two DRPs; with static and dynamic incentive tariffs are offered to the residents of SBs, respectively. The numerical outputs of the simulation of these cases are presented in Tables 10 and 11. The numerical analysis of these tables reveals a 4.85% and 10.5% reduction in total operating costs, respectively, due to the applying static- and dynamic-DRP. Moreover, the numbers presented in Tables 10 and 11 reflect that participation of SBs in DRP with a static tariff reduced their daily expenses by 3.56%, while participation in DRP with dynamic

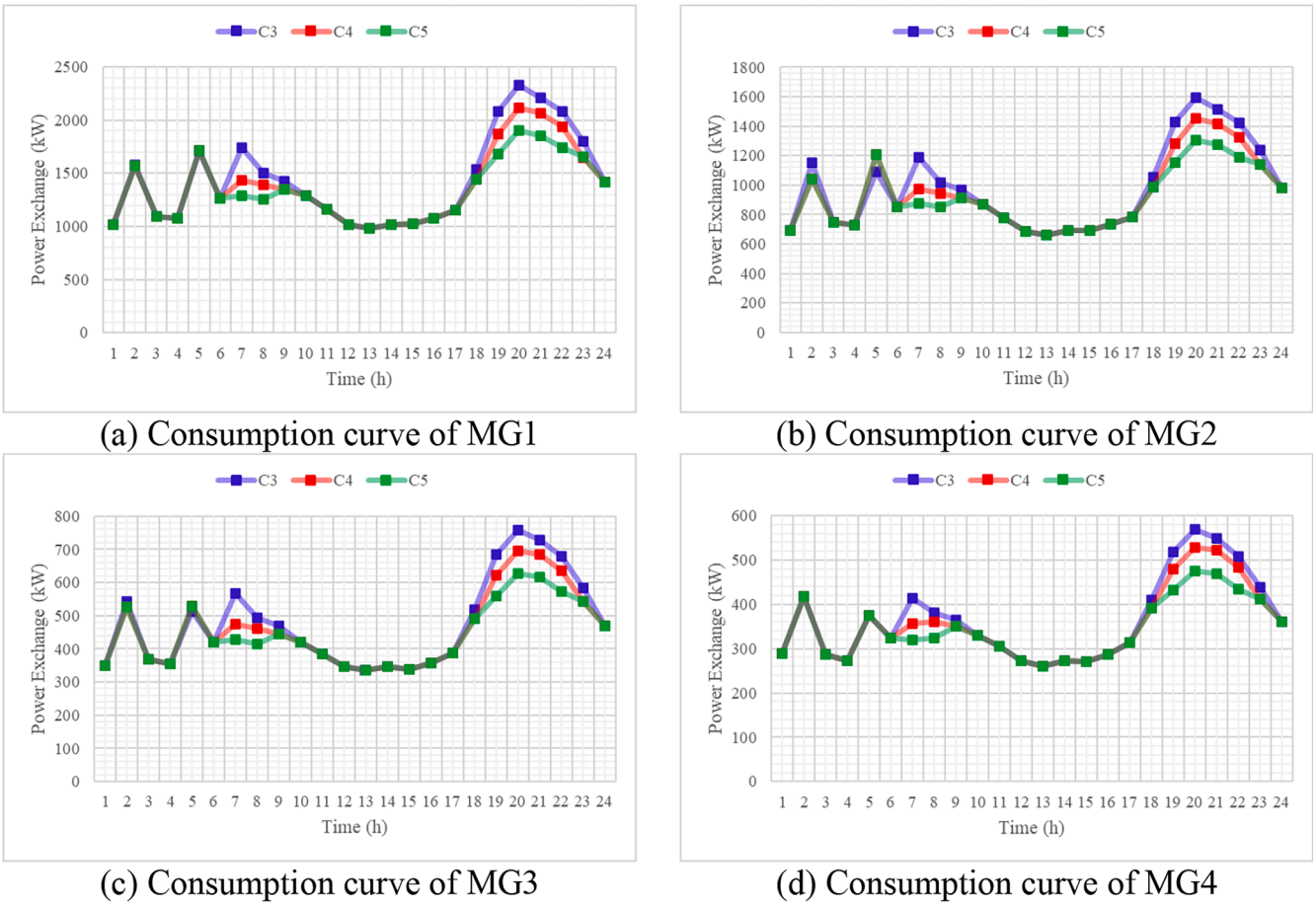

Fig. 13. The impacts of static- and dynamic-tariff DRPs on consumption curves: C3 to C5.

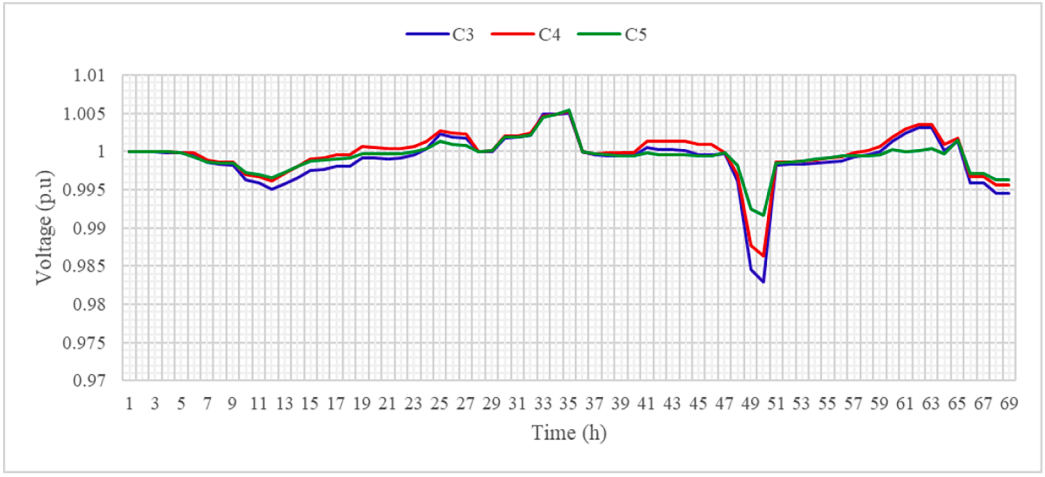

Fig. 14. The impacts of static- and dynamic-tariff DRPs on the nodal voltage: C3 to C5.

tariffs reduced their daily expenses by 4.38%. In the static-tariff DRP, SB residents are received 4 cents per kilowatt of load reduction during the high-demand periods (from 7:00 to 9:00 and from 18:00 to 23:00), while the participation rewards in the dynamic-tariff DRP are computed using Eqs. (1).

Fig. 12a-12d show the rewards associated with dynamic-tariff DRP for a SB in each MG. It should be stated that these tariffs are calculated for each SB separately according to its demand curve, and as a result, they are compatible with the behavior of its residents. According to Fig. 12a-12d, in all MGs, the highest rewards are paid between 19:00 and 21:00, when the load is at its high-demand period. In other words, in dynamic-tariff DRP, the higher the load demand, the more reward is paid to the residents to reduce their load. In this light, the comparison of tariffs in different SBs in Fig. 12a-12d illustrates that More rewards are paid in MG1 than other MGs since it has more SBs.

Fig. 13a-13d are provided to study the effect of static- and dynamic-tariff DRPs on modifying the consumption curve of MGs. Based on these figures, dynamic-tariff DRP has reduced the demand level in the peak

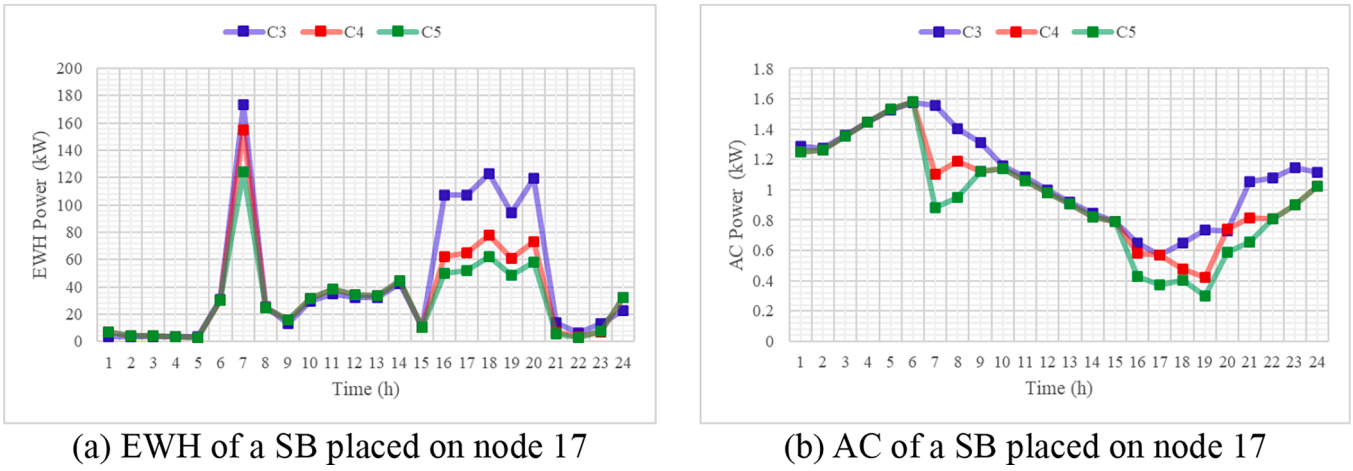

Fig. 15. The impacts of static- and dynamic-tariff DRPs on AC and EWH performance: C3 to C5.

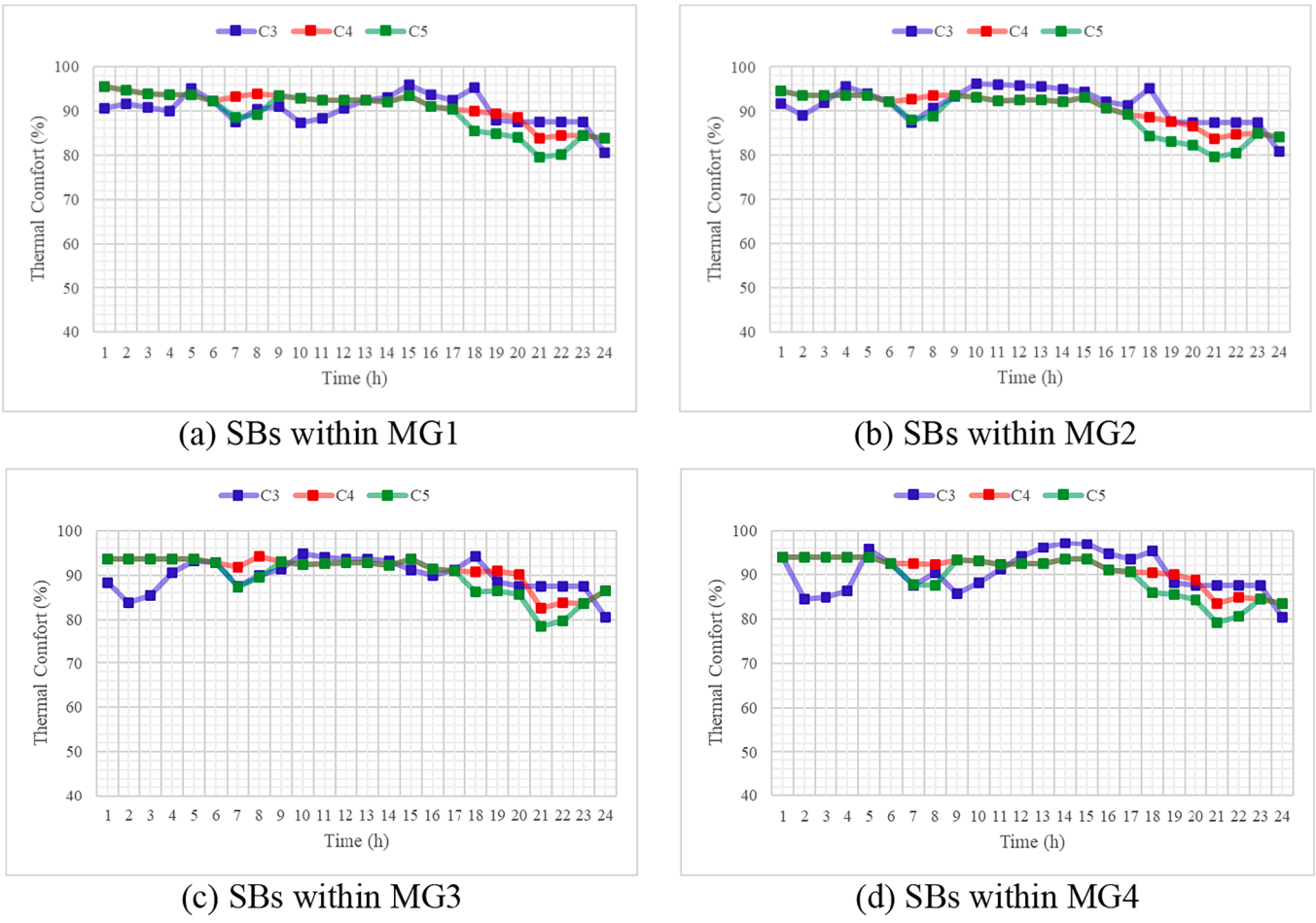

Fig. 16. Hourly TC indices obtained for SBs: C3 to C5.

period more than dynamic-tariff DRP. In addition, Fig. 14 is plotted to analyze the impact of static- and dynamic-tariff DRPs on the nodal voltage of the system at 20:00. This figure shows that both static- and dynamic-tariff DRPs improved the nodal voltage level over C3, which is due to the reduction of demand in nodes coupled to SBs. Moreover, the evaluation of the details of Fig. 14 reveals the higher impact of the dynamic-tariff DRP than the static-tariff DRP on the reduction of voltage deviations in different nodes.

The effects of DRPs on AC and EWH performance are evaluated in Fig. 15a and 15b. The analysis of the hourly performance of AC and EWH systems reflect that the implementation of DRPs has lowered the operating point of these systems during peak periods.

Hourly TC indices obtained for SBs in C3-C5 are depicted in Fig. 16a-16d, whose analysis reflects the effect of DRPs on the relative reduction of this index during both morning and evening high-demand periods. The results clearly reflect that the residents of SBs have agreed to give up part of their comfort in some hours by reducing their load in exchange for rewards. The comparison of the curves presented in Fig. 16a-16d

Table 12
Costs results for the simulation C6.

Actors	GTs ($)	BES Systems ($)	Transactions ($)		DRPs ($)	Total ($)	Profit from Selling Power to Customers ($)	
			Grid	P2P			SBs	RBs
MG1	894.95	13.25	3,125.03	−668.78	200.29	3,564.74	6,100.54	1,281.41
MG2	696.83	18.65	−259.22	329.54	100.59	886.39	4,123.60	877.00
MG3	832.38	14.92	−572.81	−208.00	27.08	93.57	1,759.44	1,269.84
MG4	533.22	8.16	404.75	67.24	14.48	1,027.84	1,091.21	1,912.13
DS	392.82	14.76	2,298.01	0.00	0.00	2,705.59	0.00	4,301.83
Sum	3,350.20	69.74	4,995.75	−480.00	342.44	8,278.12	13,074.78	9,642.21

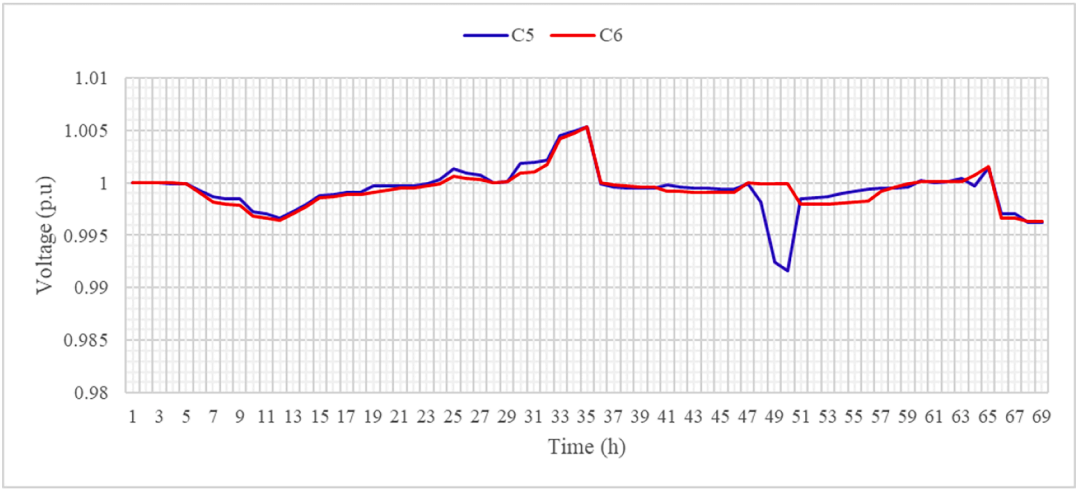

Fig. 17. The impacts of providing V2G services on the nodal voltage: C5 & C6.

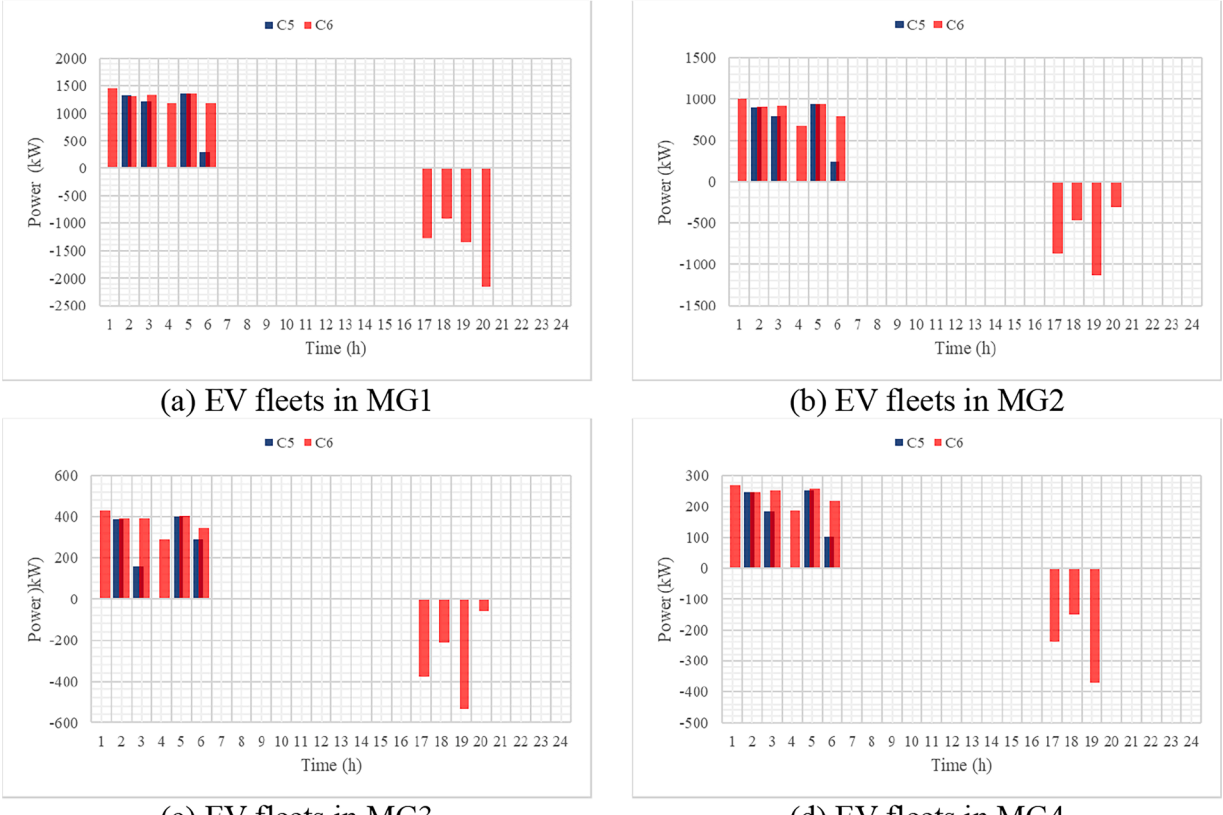

Fig. 18. EV fleets charge / discharge behavior: C5 & C6.

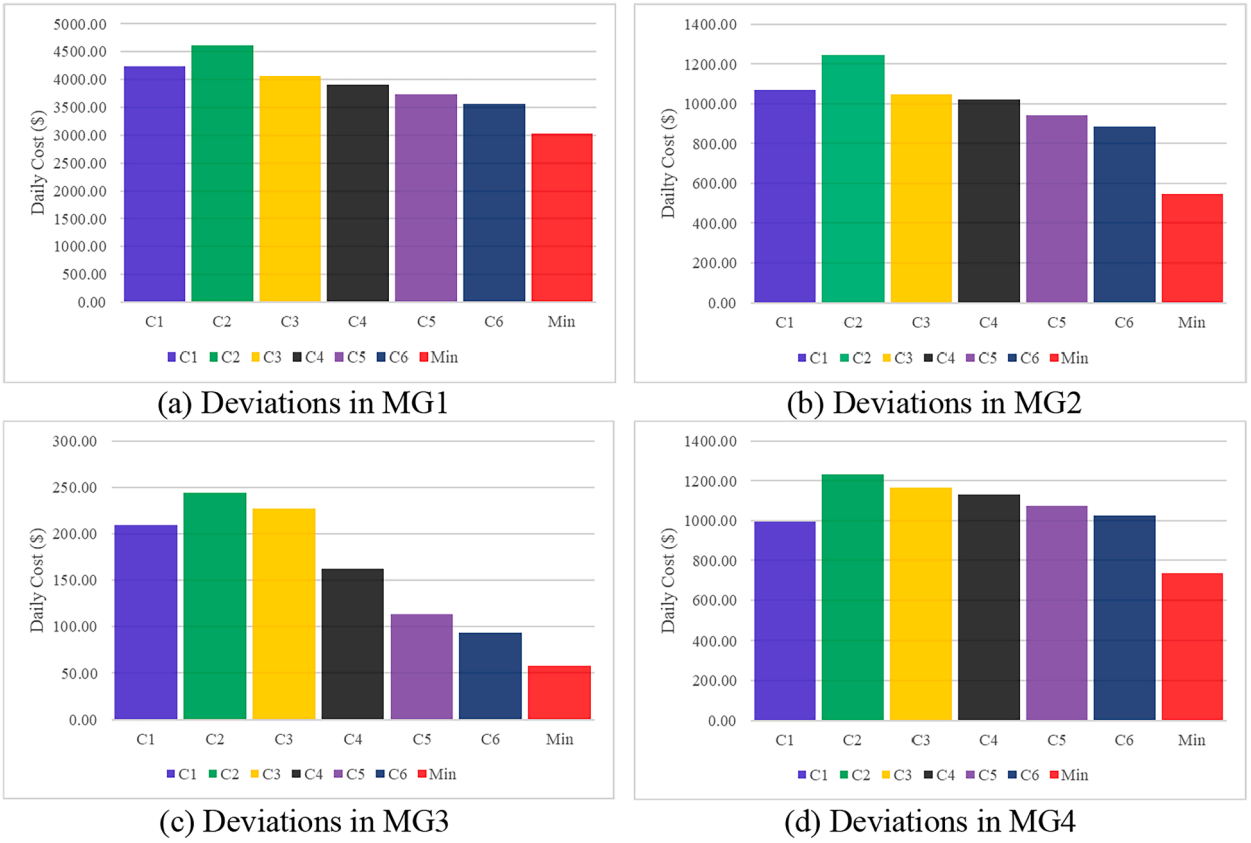

Fig. 19. Deviation of the final operating cost of MGs from their minimum operating cost: C1 to C6.

reveals that the greatest reduction of the TC index is found in C5, as in this case the residents of SBs have reduced their load more by participating in the dynamic-tariff DRP. Totally, comparing the simulation results of C4 and C5 indicates the higher impact of the dynamic-tariff DRP on modifying the consumption pattern and reducing the costs of SBs, MGs and the DS compared to the static-tariff DRP.

4.6. Simulations results of C6

In the simulation C6, EV fleets have the option to be rewarded by providing V2G services. Note that EV fleets receive this reward based on the dynamic-tariff DRP. Numerical results of Table 12 reveal that the provision of V2G services, in addition to reducing the total expenses of SBs by 7.84%, has led to a reduction of 9.26% of the total daily expenses of MGs. The benefits from providing V2G services is given to the residents of SBs since they own EVs. In Fig. 17, the effect of providing V2G services on the nodal voltage of the system at 20:00 is depicted, and its evaluation reveals the positive effect of V2G services on reducing the voltage deviations in many nodes at the high-demand hour. Fig. 18 compares the charge and discharge behavior of EV fleets of the MGs in C5 and C6. The EV fleets in all MGs have been injected power into the grid during the evening peak period and charged between 01:00 to 06:00, which is the low-demand period.

Fig. 19 depicts the deviation of the final operating cost of MGs from their minimum operating cost in C1 to C6. Comparing the results presented in these figures reveals that the highest and lowest deviations from the minimum operating cost are in C2 and C6, respectively. In the proposed cooperative game theory method, first each MG computes its minimum operating cost individually and then, its final operating cost is determined after running a cooperative game with the aim of reducing the sum of deviations of all MGs. Note that these deviations are caused by the limitations of power flow and security constraints. The results of Fig. 19 confirms that P2P power exchange, participation of SBs in DRPs and provision of V2G services significantly reduce the deviation of the final costs of MGs from their minimum cost. It should be mentioned that the proposed cooperative game theory determines the equilibrium point of DA scheduling of MGs by considering all the security and power flow restrictions with the aim of minimizing the sum of deviations and therefore prevents the creation of market power.

5. Conclusions

A three-layer cooperative game theoretic-based strategy for the DA scheduling interconnected MGs was presented in this article. In the proposed strategy, a new mechanism for designing DRP with dynamic incentive tariffs was embedded to take advantage of the potential of SBs and EV fleets to enhance technical, economic and security metrics of the operation. The scenario-based technique was used to include uncertainty in the proposed method, where the RA strategy is implemented to handle the risk of MGs scheduling. Six different cases were simulated to evaluate the validity of the proposed strategy, and the results are as follows:

- The simulation outputs showed that the implementation of cooperative game theory, despite deviating the final operating cost of MGs from their minimum operating cost, led to the achievement of an optimal equilibrium point for the DA scheduling of MGs, where all the power flow and security restrictions were met. The results reflected that the proposed cooperative game theory minimized the sum of deviations of all MGs simultaneously and thus prevented market power.
- The DA scheduling of MGs was done without and with the RA strategy, and the results reflected that the RA strategy, despite the 14.91% increase in system daily costs, significantly increased the

operational security, thus ensuring the stability of power supply in different scenarios.

- The simulation outputs mirrored that power transaction among MGs through P2P infrastructures significantly reduced their dependence on the grid. Numerical results revealed that P2P power transaction not only reduced the total daily costs of MGs by 7.97%, but also reduced system power losses.
- A new structure was introduced for the design of dynamic-tariff DRP in this article, and the simulation outputs mirrored that this structure led to more use of the potential of SBs and EV fleet to improve the technical, economic and security criteria of the system. The results reflected that the proposed dynamic-tariff DRP designer, in addition to reducing the daily expenses of SBs and MGs by 4.38% and 9.8%, respectively, led to the improvement of the voltage characteristic in the high-demand hour.

In summary, the simulation outputs strongly confirmed that the proposed three-layer strategy was able to reach an optimal equilibrium point for the DA scheduling of MGs by leveraging a cooperative game theory integrated with a linear AC power flow program, P2P power exchange, dynamic-tariff DRP implementation, and V2G service provision, where all technical, economic and security criteria are met.

Declaration of Competing Interest

The authors declare that they have no known competing financial interests or personal relationships that could have appeared to influence the work reported in this paper.

Data availability

Data will be made available on request.

References

[1] Weiss O, Pareschi G, Georges G, Boulouchos K. The Swiss energy transition: Policies to address the Energy Trilemma. Energy Policy 2021;148:111926. https://doi.org/10.1016/j.enpol.2020.111926.

[2] Al Dakheel J, Del Pero C, Aste N, Leonforte F. Smart buildings features and key performance indicators: A review. Sustain Cities Soc 2020;61:102328. https://doi.org/10.1016/j.scs.2020.102328.

[3] Chen W, Wang J, Yu G, Chen J, Hu Y. Research on day-ahead transactions between multi-microgrid based on cooperative game model. Appl Energy 2022;316:119106. https://doi.org/10.1016/j.apenergy.2022.119106.

[4] Haddadian H, Noroozian R. Multi-Microgrid-Based Operation of Active Distribution Networks Considering Demand Response Programs. IEEE Trans Sustain Energy 2019;10:1804–12. https://doi.org/10.1109/TSTE.2018.2873206.

[5] Nawaz A, Zhou M, Wu J, Long C. A comprehensive review on energy management, demand response, and coordination schemes utilization in multi-microgrids network. Appl Energy 2022;323:119596. https://doi.org/10.1016/j.apenergy.2022.119596.

[6] Imani MH, Ghadi MJ, Ghavidel S, Li L. Demand Response Modeling in Microgrid Operation: a Review and Application for Incentive-Based and Time-Based Programs. Renew Sustain Energy Rev 2018;94:486–99. https://doi.org/10.1016/j.rser.2018.06.017.

[7] Wang Z, Munawar U, Paranjape R. Stochastic Optimization for Residential Demand Response With Unit Commitment and Time of Use. IEEE Trans Ind Appl 2021;57:1767–78. https://doi.org/10.1109/TIA.2020.3048643.

[8] Ouédraogo S, Faggianelli GA, Notton G, Duchaud JL, Voyant C. Impact of electricity tariffs and energy management strategies on PV/Battery microgrid performances. Renew Energy 2022;199:816–25. https://doi.org/10.1016/j.renene.2022.09.042.

[9] Tabar VS, Ghassemzadeh S, Tohidi S. Energy management in hybrid microgrid with considering multiple power market and real time demand response. Energy 2019;174:10–23. https://doi.org/10.1016/j.energy.2019.01.136.

[10] Yu M, Hong SH, Ding Y, Ye X. An Incentive-Based Demand Response (DR) Model Considering Composited DR Resources. IEEE Trans Ind Electron 2019;66:1488–98. https://doi.org/10.1109/TIE.2018.2826454.

[11] Zhang Z, Huang Y, Chen H, Huang Q, Lee W-J. A Novel Hierarchical Demand Response Strategy for Residential Microgrid. IEEE Trans Ind Appl 2021;57:3262–71. https://doi.org/10.1109/TIA.2021.3067864.

[12] Reihani E, Motalleb M, Thornton M, Ghorbani R. A novel approach using flexible scheduling and aggregation to optimize demand response in the developing interactive grid market architecture. Appl Energy 2016;183:445–55. https://doi.org/10.1016/j.apenergy.2016.08.170.

[13] Cui H, Xia W, Yang S, Wang X. Real-time emergency demand response strategy for optimal load dispatch of heat and power micro-grids. Int J Electr Power Energy Syst 2020;121:106127. https://doi.org/10.1016/j.ijepes.2020.106127.

[14] Thirunavukkarasu GS, Seyedmahmoudian M, Jamei E, Horan B, Mekhilef S, Stojcevski A. Role of optimization techniques in microgrid energy management systems—A review. Energy Strateg Rev 2022;43:100899. https://doi.org/10.1016/j.esr.2022.100899.

[15] Kermani M, Adelmanesh B, Shirdare E, Sima CA, Carnì DL, Martirano L. Intelligent energy management based on SCADA system in a real Microgrid for smart building applications. Renew Energy 2021;171:1115–27. https://doi.org/10.1016/j.renene.2021.03.008.

[16] Moazeni F, Khazaei J. Dynamic economic dispatch of islanded water-energy microgrids with smart building thermal energy management system. Appl Energy 2020;276:115422. https://doi.org/10.1016/j.apenergy.2020.115422.

[17] Ouammi A. Peak Loads Shaving in a Team of Cooperating Smart Buildings Powered Solar PV-Based Microgrids. IEEE Access 2021;9:24629–36. https://doi.org/10.1109/ACCESS.2021.3057458.

[18] Ouammi A. Peak load reduction with a solar PV-based smart microgrid and vehicle-to-building (V2B) concept. Sustain Energy Technol Assessments 2021;44:101027. https://doi.org/10.1016/j.seta.2021.101027.

[19] Rezaei N, Khazali A, Mazidi M, Ahmadi A. Economic energy and reserve management of renewable-based microgrids in the presence of electric vehicle aggregators: A robust optimization approach. Energy 2020;201:117629. https://doi.org/10.1016/j.energy.2020.117629.

[20] Kharrich M, Mohammed OH, Alshammari N, Akherraz M. Multi-objective optimization and the effect of the economic factors on the design of the microgrid hybrid system. Sustain Cities Soc 2021;65:102646. https://doi.org/10.1016/j.scs.2020.102646.

[21] Mansoor M, Stadler M, Auer H, Zellinger M. Advanced optimal planning for microgrid technologies including hydrogen and mobility at a real microgrid testbed. Int J Hydrogen Energy 2021;46:19285–302. https://doi.org/10.1016/j.ijhydene.2021.03.110.

[22] Lee LY, Choi SG. Power Purchase Cost Minimization in Radial Microgrid Network with Linear Programming. 2020 Int Conf Inf Commun Technol Converg 2020:1805–7. https://doi.org/10.1109/ICTC49870.2020.9289431.

[23] Mehran K. Integrated active/reactive power scheduling of interdependent microgrid and EV fleets based on stochastic multi-objective normalised normal constraint. IET Gener Transm Distrib 2020;14:2055-2064(9).

[24] Garmabdari R, Moghimi M, Yang F, Gray E, Lu J. Multi-objective energy storage capacity optimisation considering Microgrid generation uncertainties. Int J Electr Power Energy Syst 2020;119:105908. https://doi.org/10.1016/j.ijepes.2020.105908.

[25] Hemmati M, Mirzaei MA, Abapour M, Zare K, Mohammadi-ivatloo B, Mehrjerdi H, et al. Economic-environmental analysis of combined heat and power-based reconfigurable microgrid integrated with multiple energy storage and demand response program. Sustain Cities Soc 2021;69:102790. https://doi.org/10.1016/j.scs.2021.102790.

[26] Godazi Langeroudi AS, Sedaghat M, Pirpoor S, Fotouhi R, Ghasemi MA. Risk-based optimal operation of power, heat and hydrogen-based microgrid considering a plug-in electric vehicle. Int J Hydrogen Energy 2021;46:30031–47. https://doi.org/10.1016/j.ijhydene.2021.06.062.

[27] Li L. Coordination between smart distribution networks and multi-microgrids considering demand side management: A trilevel framework. Omega 2021;102:102326. https://doi.org/10.1016/j.omega.2020.102326.

[28] Zhou Z, Xiong F, Huang B, Xu C, Jiao R, Liao B, et al. Game-Theoretical Energy Management for Energy Internet With Big Data-Based Renewable Power Forecasting. IEEE Access 2017;5:5731–46. https://doi.org/10.1109/ACCESS.2017.2658952.

[29] Javanmard B, Tabrizian M, Ansarian M, Ahmarinejad A. Energy management of multi-microgrids based on game theory approach in the presence of demand response programs, energy storage systems and renewable energy resources. J Energy Storage 2021;42:102971. https://doi.org/10.1016/j.est.2021.102971.

[30] Fu Y, Zhang Z, Li Z, Mi Y. Energy Management for Hybrid AC/DC Distribution System With Microgrid Clusters Using Non-Cooperative Game Theory and Robust Optimization. IEEE Trans Smart Grid 2020;11:1510–25. https://doi.org/10.1109/TSG.2019.2939586.

[31] Aguila-Leon J, Chiñas-Palacios C, Garcia EXM, Vargas-Salgado C. A multimicrogrid energy management model implementing an evolutionary game-theoretic approach. Int Trans Electr Energy Syst 2020;30:e12617.

[32] Vieira G, Zhang J. Peer-to-peer energy trading in a microgrid leveraged by smart contracts. Renew Sustain Energy Rev 2021;143:110900. https://doi.org/10.1016/j.rser.2021.110900.

[33] Wang Z, Yu X, Mu Y, Jia H, Jiang Q, Wang X. Peer-to-Peer energy trading strategy for energy balance service provider (EBSP) considering market elasticity in community microgrid. Appl Energy 2021;303:117596. https://doi.org/10.1016/j.apenergy.2021.117596.

[34] Qiu D, Xue J, Zhang T, Wang J, Sun M. Federated reinforcement learning for smart building joint peer-to-peer energy and carbon allowance trading. Appl Energy 2023;333:120526. https://doi.org/10.1016/j.apenergy.2022.120526.

[35] Zhao J, Wang W, Guo C. Hierarchical optimal configuration of multi-energy microgrids system considering energy management in electricity market environment. Int J Electr Power & Energy Syst 2023;144:108572. https://doi.org/10.1016/j.ijepes.2022.108572.

[36] Dey B, Raj S, Mahapatra S, Márquez FPG. Optimal scheduling of distributed energy resources in microgrid systems based on electricity market pricing strategies by a

novel hybrid optimization technique. Int J Electr Power & Energy Syst 2022;134:107419. https://doi.org/10.1016/j.ijepes.2021.107419.
[37] Jafarpour P, Nazar MS, Shafie-khah M, Catalão JPS. Resiliency assessment of the distribution system considering smart homes equipped with electrical energy storage, distributed generation and plug-in hybrid electric vehicles. J Energy Storage 2022;55:105516. https://doi.org/10.1016/j.est.2022.105516.
[38] Mansouri SA, Ahmarinejad A, Nematbakhsh E, Javadi MS, Esmaeel Nezhad A, Catalão JPS. A sustainable framework for multi-microgrids energy management in automated distribution network by considering smart homes and high penetration of renewable energy resources. Energy 2022::123228. https://doi.org/10.1016/j.energy.2022.123228.
[39] Vilaisarn Y, Rodrigues YR, Abdelaziz MMA, Cros J. A Deep Learning Based Multiobjective Optimization for the Planning of Resilience Oriented Microgrids in Active Distribution System. IEEE Access 2022;10:84330–64. https://doi.org/10.1109/ACCESS.2022.3197194.
[40] Guo S, Li P, Ma K, Yang B, Yang J. Robust energy management for industrial microgrid considering charging and discharging pressure of electric vehicles. Appl Energy 2022;325:119846. https://doi.org/10.1016/j.apenergy.2022.119846.
[41] Komeili M, Nazarian P, Safari A, Moradlou M. Robust optimal scheduling of CHP-based microgrids in presence of wind and photovoltaic generation units: An IGDT approach. Sustain Cities Soc 2022;78:103566. https://doi.org/10.1016/j.scs.2021.103566.
[42] Saeian H, Niknam T, Zare M, Aghaei J. Coordinated optimal bidding strategies methods of aggregated microgrids: A game theory-based demand side management under an electricity market environment. Energy 2022;245:123205. https://doi.org/10.1016/j.energy.2022.123205.
[43] Huang C, Zhang M, Wang C, Xie N, Yuan Z. An interactive two-stage retail electricity market for microgrids with peer-to-peer flexibility trading. Appl Energy 2022;320:119085. https://doi.org/10.1016/j.apenergy.2022.119085.
[44] Hussain MS, Kazmi SAA, Khan ZA, Alghassab M, Altamimi A. Hierarchical Energy Management System With a Local Competitive Power Market for Inter-Connected Multi-Smart Buildings. IEEE Access 2022;10:19493–506. https://doi.org/10.1109/access.2022.3150327.
[45] Akbari-Dibavar A, Mohammadi-Ivatloo B, Zare K, Anvari-Moghaddam A. Optimal Scheduling of a Self-Healing Building Using Hybrid Stochastic-Robust Optimization Approach. IEEE Trans Ind Appl 2022;58:3217–26. https://doi.org/10.1109/tia.2022.3155585.
[46] Xu Y-P, Liu R-H, Tang L-Y, Wu H, She C. Risk-averse multi-objective optimization of multi-energy microgrids integrated with power-to-hydrogen technology, electric vehicles and data center under a hybrid robust-stochastic technique. Sustain Cities Soc 2022;79:103699. https://doi.org/10.1016/j.scs.2022.103699.
[47] Roccotelli M, Mangini AM, Fanti MP. Smart District Energy Management With Cooperative Microgrids. IEEE Access 2022;10:36311–26. https://doi.org/10.1109/access.2022.3163724.
[48] Saif A, Khadem SK, Conlon M, Norton B. Impact of Distributed Energy Resources in Smart Homes and Community-Based Electricity Market. IEEE Trans Ind Appl 2022:1–11. https://doi.org/10.1109/tia.2022.3202756.
[49] Lee ZE, Zhang KM. Regulated peer-to-peer energy markets for harnessing decentralized demand flexibility. Appl Energy 2023;336:120672. https://doi.org/10.1016/j.apenergy.2023.120672.
[50] May R, Huang P. A multi-agent reinforcement learning approach for investigating and optimising peer-to-peer prosumer energy markets. Appl Energy 2023;334:120705. https://doi.org/10.1016/j.apenergy.2023.120705.
[51] Zhang R, Li X, Fu L, Jiang T, Li G, Chen H. Network-aware energy management for microgrids in distribution market: A leader-followers approach. Appl Energy 2023;332:120522. https://doi.org/10.1016/j.apenergy.2022.120522.
[52] Yu Y, Li G, Liu Y, Li Z. V2V Energy Trading in Residential Microgrids Considering Multiple Constraints via Bayesian Game. IEEE Trans Intell Transp Syst 2023:1–12. https://doi.org/10.1109/TITS.2023.3250649.
[53] Jin X, Jia H, Mu Y, Li Z, Wei W, Yu X, et al. A Stackelberg Game based Optimization Method for Heterogeneous Building Aggregations in Local Energy Markets. IEEE Trans Energy Mark Policy Regul 2023:1–13. https://doi.org/10.1109/TEMPR.2023.3251325.
[54] Zou Y, Xu Y, Zhang C. A Risk-Averse Adaptive Stochastic Optimization Method for Transactive Energy Management of a Multi-Energy Microgrid. IEEE Trans Sustain Energy 2023:1–12. https://doi.org/10.1109/TSTE.2023.3240184.
[55] Alfaverh F, Denai M, Sun Y. A Dynamic Peer-to-Peer Electricity Market Model for a Community Microgrid with Price-Based Demand Response. IEEE Trans Smart Grid 2023:1. https://doi.org/10.1109/TSG.2023.3246083.
[56] Mansouri SA, Rezaee Jordehi A, Marzband M, Tostado-Véliz M, Jurado F, Aguado JA. An IoT-enabled hierarchical decentralized framework for multi-energy microgrids market management in the presence of smart prosumers using a deep learning-based forecaster. Appl Energy 2023;333:120560. https://doi.org/10.1016/j.apenergy.2022.120560.
[57] Zhou J, Xu Z. Optimal sizing design and integrated cost-benefit assessment of stand-alone microgrid system with different energy storage employing chameleon swarm algorithm: A rural case in Northeast China. Renew Energy 2023;202:1110–37. https://doi.org/10.1016/j.renene.2022.12.005.